uc3m | Universidad Carlos III de Madrid

Bachelor's Degree in Aerospace Engineering
2018

*Bachelor Thesis*

# Parametric study in modeling orthogonal machining of CFRP

Bárbara Perucha Calvo

Tutor
Víctor Criado del Álamo

**Abstract**

Composite materials machining is a field in which theoretical knowledge is still being studied. However, these materials have revolutionized some industries as the aeronautical due to their exceptional mechanical properties and its lightness. In order to analyse possible post-manufacturing process FEM has become popular. Models are created with the purpose of predicting the possible damage and forces required. This thesis shows the process followed to develop one of those models in the software LS-DYNA. An orthogonal cut is simulated. The validation given experimental data of the same orthogonal cut is justified. One of the main problems is also implemented in the model: delamination of the composite plies. The advantages of numerical models are exposed by analysing different cases and results such as stress and pressure contours in a less amount of time and with a lower cost.

# Contents

# List of Figures

# List of tables

**Acronyms and abbreviations**

- FEM: Finite Element Method
- FRP: fibre reinforces polymer
- CFRP: carbon fibre reinforced polymer
- GFRP: glass fibre reinforced polymer
- $\rho$: density
- E: Young's/elastic modulus
- $\nu$: Poisson's ratio
- $G_{ij}$: Shear modulus ij
- $\sigma$: stress
- $X_T$: longitudinal tensile strength
- $X_C$: longitudinal compressive strength
- $Y_T$: transverse tensile strength
- $Y_C$: transverse compressive strength
- $S_{ij}$ shear strength
- $G_{I/IIc}$: energy release rate for mode I/II
- $u_{ND}$: ultimate displacement in normal direction
- $u_{TD}$: ultimate displacement in tangential direction
- $S$: peak traction in normal direction
- $T$: peak traction in tangential direction
- $E_N$: stiffness normal to the plane of the cohesive element
- $E_T$: stiffness in the plane of the cohesive element

# 1 Introduction

In this section it is explained the main reasons which conducted to this project, the goals to be achieved and the development process followed.

## 1.1 Motivation

In the last years, the use of composite materials in the aerospace field has increased up to the point that, nowadays, the aerospace market is one of the largest and arguably the most important to the composites industry. Commercial aircraft, military craft, helicopters, business jets, general aviation aircraft and space craft all make substantial use of composites, both inside and outside.

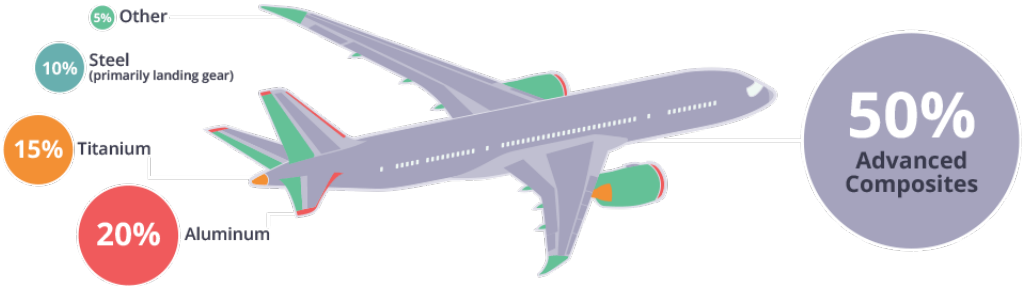


**Figure** 1: Materials in Boeing-787 [1]

This increase is related to the replacement of traditional materials such as metals, due to the improved characteristics of composite materials. Regarding the strength and stiffness, reinforced composite materials are better, especially as the strain before fracture decreases compared to the metals of the same strength. However, the main advantage of the composite materials is the weight, when considering the elastic module per unit of mass (named as specific module) and the strength per unit of mass (specific strength). In case of a higher specific module and specific strength (composite materials), the weight can be reduced, what is very relevant to the aerospace field. To sum up, composite materials are characterized by having exceptional mechanical properties and a very low density compared to traditional materials.

On the other hand, there are also some disadvantages, mainly at the time for shaping and machining these materials. As there is not a lot of information related to the behaviour of these materials, most of the processes are performed after experimental tests, leading to an increase of costs.

At this moment it is still very difficult to relate the experimental results in these tests with the theoretical knowledge of the material, so that the prediction through theoretical methods becomes complicated. However, a good option to predict the behaviour apart from the experiments is to simulate the process based on a numerical method. Although the same problems as before appear, a parametric study can lead to a validated model for a given material and process.

This thesis studies the behaviour, under a cutting process, of a composite material by means of a finite element method. The results will be validated with experimental tests perform in the same conditions and, after the validation, an analysis of different cases will be done. Through out all the possible options, this project focuses in CFRP (Carbon Fibre Reinforced Plastic), as it is the most common composite in the aerospace field. Orthogonal cutting is the specific process of this study, because of its simplicity and the fact that the results give a significant approach to the composite behaviour. The software selected for this project is named LS-DYNA.

## 1.2 Objectives

The main goal of this project is to validate the numerical model proposed to simulate the orthogonal cutting to a CFRP. In order to achieve this goal, the numerical results are compared with experimental results at the same conditions.

An analysis of the chosen software accuracy, easiness and sensitivities is performed. The results are considered at different cutting conditions, delamination, as well as mesh sensitivities are studied. Based on this, the second objective is to determine for which purposes the software simulations are valid as well as established their limitations. In the end, it is concluded if the selected software is a good option and, therefore, it is suggested to create more models of different manufacturing processes or, on the contrary, if there are improvements to be made before this type of models are optimized.

## 1.3 Stages of development

First of all, a research process is done in order to find out the state of the art related to the manufacturing processes of materials and their numerical simulations.

After that, when building the model in LS-DYNA there exist fixed parameters, such as the material properties. However, the software offers different options to simulate composite materials, based on the criteria to perform the damage. This will be explained in Section 3

In the comparison, the material of the tool must have the same properties as the ones set in LS-DYNA. Moreover, tool geometry as well as velocity and depth of cut must be the same as in the experimental tests.

Once the validation is reached throughout the contact forces, different cases of the same material and cutting process are studied, and an analysis of the tool damage and the possible delamination in the composite is done.

## 1.4 Means

Currently, in order to simplify the experimental time and its costs, Finite Element Methods (FEM) are used. They allow to solve complex computations in a fast and simple way, reducing the number of experiments. The software used for the simulations is *LS-DYNA*, a multiphysics, finite element software.

Besides, the access to a different bachelor thesis is required, made parallel to this one, in which the experimental behaviour of the same material is analysed. From this thesis the contact forces are extracted in order to validate the model and the results are also compared.

## 1.5 Thesis structure

The report of this project is divided into the following sections:

- Section 1.-Introduction: a brief introduction is done, exposing the topic of the thesis. The motivation, main objectives, stages of development and means are also explained in this section.
- Section 2.- Theoretical Approach: all the concepts related to this project are explained in this section, always from a useful point of view, so that in case that the reader is not familiar with some concept it facilitates the project understanding. Moreover, the state of the art of the manufacturing processes and numerical models related to composite materials can be found here.
- Section 3.- Numerical model: a description of all the steps taken to build the numerical model in LS-DYNA is done here, justifying the elections and showing some alternatives. The factors varied during the parametric study are depicted. Finally a mesh sensitivity analysis is performed and mesh influence is examined, justifying the mesh election.
- Section 4.- Results: first a comparison between the principal forces obtained in the experimental test and the ones from the numerical model is done in order to validate the model. An analysis of different cases for the same manufacturing process is performed: numerical principal force for different cutting conditions and numerical thrust force, stresses, delamination, and tool damage are studied.
- Section 5.- Socio-economic impact and legal framework: a budget of the project as well as its socio-economic and legal impact is shown in this section.
- Section 6.- Conclusions and future projects: the conclusions achieved at the end of this project are stated, as well as possible future projects related to the same topic.

# 2 Theoretical Approach

In this section composite materials are defined, including properties and applications. The main equations, such as failure criteria and anisotropic properties of composite materials are presented. Related to the manufacturing process, the main concepts are explained and the state of the art of these processes applied to composite materials is exposed. This chapter also contains the concept of Finite Element Method. Finally, the experiment performed in order to validate the model is described, as well as, briefly, the machine and development.

## 2.1 Aerospace materials

In the aerospace field the importance of the materials is key to the design of the aircraft, the election affects many aspects to be considered, such as:

- Purchase cost of a new aircraft.
- Cost of structural upgrades to existing aircraft.
- Design options for the airframe, structural components and engines.
- Fuel consumption of the aircraft (light-weighting).
- Operational performance of the aircraft (speed, range and payload).
- In-service maintenance (inspection and repair) of the airframe and engines.
- Safety reliability and operational life of the airframe and engines.
- Disposal and recycling of the aircraft and the end-of-life.

Sometimes a compromise between these aspects is required, as the optimum material for each of them can be different. Therefore, when designing an aircraft, there is a list of selection factors to be fulfilled that helps in the election of the aerospace structural materials, some of which are shown below:

- The choice is governed by the design, function, loads, and environmental service conditions of the structure.
- There exists "safety-critical structures", structures that can result in loss of the aircraft when they fail: fuselage, wings, landing gear, empennage, gas turbine engines (blades, discs...). Most of the safety-critical structures require a combination of high stiffness, strength, fracture toughness, fatigue endurance and corrosion resistance.
- Damage tolerance and durability must be over the aircraft design life:
  – Military fighter aircraft: 8000-14000 flight hours, 15-40 years.
  – Large commercial airliner: 30000-60000 flight hours, 25-30 years.

After this overview of the aerospace requirements, in Figure 2 it can be observed a timeline of the main aerospace materials and when they were introduced in the industry.

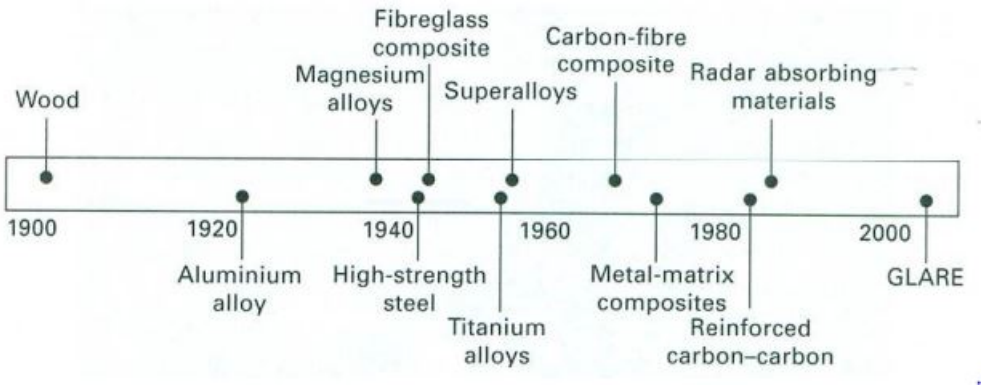


**Figure** 2: Aerospace materials in the industry [2]

As it can be seen, composite materials belong to the list of materials used in the aerospace field. However they are one of the most recent to be used and, at the beginning, as most of the new materials, they were applied only in the military sector. Therefore it can be assume that they fulfilled the requirements to be used in this sector, and even surpassed some of the older materials. In the following sections a deeper approach to composites is done.

## 2.2 Composite materials

Composite materials are commonly defined as a combination of two or more constituent materials, with significantly different physical or chemical properties, which remain separate and distinct on a macroscopic or microscopic level within the finished structure. Usually a synergistic effect in one or more properties is observed, meaning that the overall performance of the material should be better than the separate components for a particular application.

Considering the previous definition, the most common composite material can be considered to be the concrete, as a combination of cement and aggregate. However, in this thesis, among all the different composite materials, when referring to them it is meant to a specific kind known as Fibre-Reinforced Polymers (FRPs).

### 2.2.1 FRPs properties and classification

Regarding the specific characteristics of these materials with respect to others, FRPs are especially interesting for the aerospace industry due to one main reason: the benefits of the excellent specific strength and specific stiffness properties (strength and stiffness per unit weight) of composites lead to a lightweight of the structural design, one of the main concerns of this industry. A comparative between metals and composites can be appreciated in Figure 3. where UD stand for unidirectional. Furthermore, the laminated nature of high performance composite materials enables the designer to optimize mechanical properties by orientating the fibre direction with the primary load paths. Other advantages of fibre reinforced plastics, such as the relative ease to manufacture complex shapes, and their excellent fatigue and corrosion resistance, have made FRP composites increasingly

attractive in many sectors.

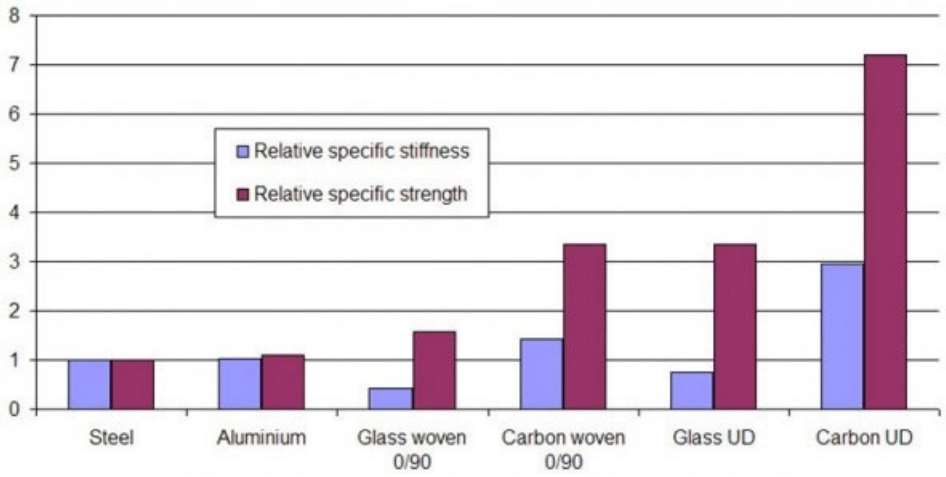


**Figure** 3: Specific stiffness and strength in different materials [3]

Another important difference with the previous materials used in aerospace is that composites absorb impact energy by damage modes rather than local plastic deformation. This means failure is typically sudden and catastrophic without any prior warning that the structure has been overloaded.

Once the main characteristics are stated, it is important to focus in the composition of these materials, as it can provide a qualitative understanding of their behaviour. As said before FRPs are a combination of different materials, the continuous phase that surrounds the other constituent and binds it into a composite material is the matrix (blue part in Figure 4). On the other hand, continuous and straight fibres (shown with colour red in Figure 4) act as reinforcement. Both constituents together form individual plies, which typically are embedded in a host polymer matrix, laminated layer-by-layer until reaching the final material.

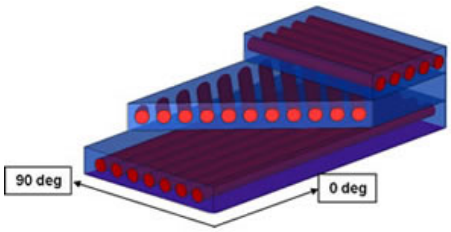


**Figure** 4: Fibre directions [2]

A good bonding between the matrix and the fibres is required. The main function of the reinforcement is to provide mechanical and physical properties to enhance the mechanical performance of the material; the fibres are the ones in charge of carrying the loads applied. The factors derive from the fibres that affect the physical an mechanical properties are: the size, distribution, shape, concentration and orientation of the fibres. On the other hand, regarding the matrix

function, it shapes the component, transfers the load to the fibres, separates the reinforcement in order to prevent failure of adjacent fibres if one fails, protects the fibre from the environment and keeps the orientations.

The alignment control of fibres is known as anisotropy. It can also be observed in the previous figure, each of the three plies is aligned in one direction. This allows several combinations which can be selected with the aim of optimizing the mechanical properties based on the primary load paths, as explained before. The most typical orientations are 0, ± 45 and 90 degrees. Laminated composites must always be symmetric with respect to their middle plane. This configuration can be easily understood in Figure 5. This picture shows a symmetric composite of the form $[0, +45, -45, 90]_s$.

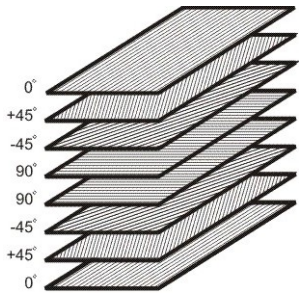


**Figure** 5: Composite layer [2]

The specific composite analysed in this thesis has also a symmetric composition. The orientation of the fibres is expressed as $[(+45, -45, 90, 0)x3]_s$ which means that the composite material is composed by 24 plies.

When composites are extremely anisotropic, with hard interphases (large gradient in composition and properties) and designed for structural application,such as the FRPs, they are named advanced composites.

The properties of the composites are a function of the constituents phases, their relative amounts, and the geometry of the dispersed phase. For this reason, in order to give an accurate approach of some of the properties, a previous classification of FRPs must be done.

The most general classification can be done as a function of the matrix (polymeric, ceramic, metallic, and organic) and reinforcement (particles, fibres, structural). As the name implies, FRPs are composed by fibre reinforcement and polymeric matrix. Some advantages of these composite materials are:

- Good specific mechanical performance
- Good fatigue performance
- Low weight
- Custom design
- Dimensional stability
- High chemical resistance
- No corrosion problems
- Good fire behavior
- Reduction in number of parts

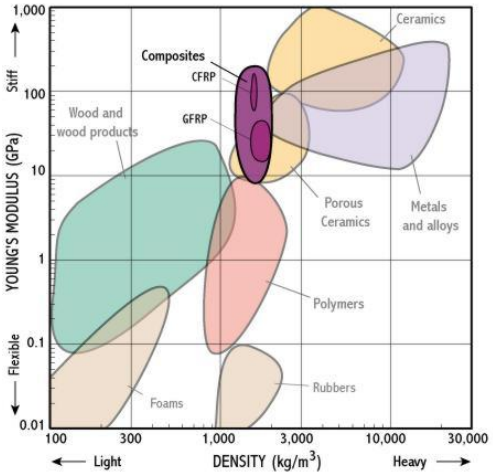


**Figure** 6: Materials distribution [4]

On the other hand, some disadvantages of FRPs are:

- Costly programs for evaluation, and certification of structures
- Costly investments for installations and equipment
- High material cost
- Water entry in sandwich structures
- Low impact resistance
- Additional protection for erosion
- Low thermal conductivity
- Additional protection for lightning
- Low recyclability

Once FRPs are placed among all the other different composite materials and their properties are generally descibed, a more detailed classification of FRPs can be done and therefore, the properties can be more accurate defined.

Regarding polymers matrices, GFRPs and CFRPs (glass and carbon fibres reinforced polymers, respectively) are noteworthy. Since the development of these two fibres in the 1950's the aerospace industry is steadily moving towards "all-composite" civil aircraft. Depending on the different materials of fibres and polymeric matrices, the RFPs can be easily classified. The most common fibre and resin types used today are depicted in this section with some of the most important characteristics.

| Glass | Carbon | Aramid – Kevlar™ |
|---|---|---|
| Diameter ≈ 10 mm | Diameter ≈ 8 mm | Stiffness ≈ 125GPa in tension |
| Strength >3GPa due to lack of defects on small diameter fibre | Strength >5GPa due to highly aligned planes of graphite | Strength >3GPa because of highly aligned linear polymer chains |
| Stiffness ≈ 70 GPa for cheaper E-glass and 85 GPa for moreexpensive R- or S- Glass | Stiffness ≈ 160-700 GPa but 230-400 GPa is the usual | Much weaker and less stiff in compression as linear polymer chains come apart |
| Susceptible to environmental attack and fatigue | Not susceptible to degradation by chemicals and good in fatigue | Susceptible to degradation by UV light and moisture |
| Fibres need silane treatment to bond well to matrix | Fibres bond well with surface treatment | Fibres do not bond well at all leading to a weak fibre/matrix interface |
| Used in boats, wind turbine blades and other cost critical applications | Expensive material cost limits use to high performance applications were the higher mechanical properties are justified i.e. Racecars, aerospace etc. | Weak interface gives excellent energy absorption. Thus used for bullet-proof vests, helmets and impact protection on aircraft |

**Table** 1: Fibres types [5]

| Phenolic | Polyester | Epoxy |
|---|---|---|
| First modern resin | Most commonly used matrix | Most common in aerospace |
| Tends to be brittle | Resin can be quite tough | Can be made quite tough |
| Wets out fibres badly | Wets out reinforcement very well | Wets out reinforcements very well |
| Good chemical, heat and fire resistance and don't produce toxic gases in a fire | Poor chemical resistance and burns very easily | Good chemical resistance but will burn |
| Thus used in aircraft interiors | Very cheap resin used alongside glass fibres in boat hulls, wind turbine blades and other cost critical applications | Generally used in combination with carbon fibre for high performance, lightweight applications |

**Table** 2: Matrix types [5]

Finally, the specific FRP used in the experimental test, and therefore in the simulated model, is a carbon fibre reinforced with an epoxy polymeric matrix. In comparison to glass fibre, it is lighter and stronger. Some disadvantages are the cost (also higher than GFRP) and its high conductivity. It is considered as a high performance material with exceptional mechanical properties very adequate for the aerospace field due to its lightness.

### 2.2.2 Failure criteria and equations

As said before, composites are anisotropic, or more specifically, orthotropic materials. This means that their properties differ along three mutually-orthogonal axes of rotational symmetry. Defining the local axes with the subindex 1, 2, 3 and with respect to the laminate as shown in Figure 7; the elastic modulus and poison ratio in every direction can be obtained through the Equation 1.

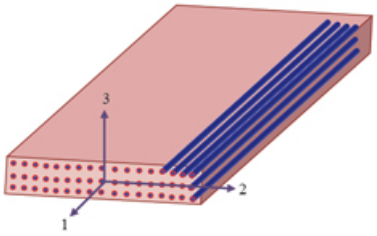


**Figure** 7: Local axes [2]

$$E_i \nu_{ij} = E_j \nu_{ji}, \quad j, i = 1...3, \quad i \neq j \qquad (1)$$

Due to the fact that for the FEM it has been used a software in which the composites materials are already implemented, by knowing the properties of the composite material oriented to one direction and changing the direction in the software, it computes the rest of the different properties. Therefore, in this thesis it is not explained in depth the equations to obtain the properties as it is not relevant for the development of the work done.

In order to determine when there is a failure in the composite material, different criteria can be applied.The most typical ones are briefly explained below:

- Tresca

  Considering the stress in every principal direction, which can be named $\sigma_1 \geq \sigma_2 \geq \sigma_3$. Then it can be stated that the failure is reached when $\tau_{max} \geq \sigma_Y/2$, where $\sigma_Y$ is the yielding stress. Finally, $\tau_{max}$ is defined in Equation 2.

$$\tau_{max} = (\sigma_1 - \sigma_3)/2 \qquad (2)$$

- Von Mises

  This criteria can be considered as an improved version of the previous one. Considering again $\sigma_1 \geq \sigma_2 \geq \sigma_3$, and defining a variable as Von Mises stress, $\sigma_{vM}$, failure appears when Equation 3 is fulfilled.

$$\sigma_{vM} = \sqrt{\frac{(\sigma_1 - \sigma_2)^2 + (\sigma_2 - \sigma_3)^2 + (\sigma_3 - \sigma_1)^2}{2}} \geq \sigma_Y \qquad (3)$$

- Hashin - Rotem criterion [6]

  This is a very important criterion to define the failure of fibrous composite materials, as it is the first one which considers two mechanisms of failure: fibre and matrix failure. Here it is shown the first proposal, done in 1973,

although there are others, including modifications for 3D and 2D cases. Failure is predicted when one of the following equations are satisfied:

- fibre failure in tension $\sigma_{11} = X_T \qquad (\sigma_{11}, X_T > 0)$
- fibre failure in compression $-\sigma_{11} = X_C \qquad (\sigma_{11} < 0, X_C > 0)$
- Matrix failure mode in tension $(\frac{\sigma_{22}}{Y_T})^2 + (\frac{\sigma_{12}}{S})^2 = 1$
- Matrix failure mode in compression $(\frac{\sigma_{22}}{Y_C})^2 + (\frac{\sigma_{12}}{S})^2 = 1$

- Chang - Chang [7]

  The Chang - Chang criteria, as the Hashin, also differentiates the two mechanisms, and it is given as follows:

  - fibre failure in tension

    $$\sigma_{aa} > 0 \quad \text{then} \quad e_f^2 = (\tfrac{\sigma_{aa}}{X_t})^2 + \beta(\tfrac{\sigma_{ab}}{S_c}) - 1 \begin{cases} \geq 0 \ \ failed \\ < 0 \ \ elastic \end{cases}$$

    $$E_a = E_b = G_{ab} = \nu_{ba} = \nu_{ab} = 0$$

  - Fibre failure in compression

    $$\sigma_{aa} < 0 \quad \text{then} \quad e_c^2 = (\tfrac{\sigma_{aa}}{X_c})^2 - 1 \begin{cases} \geq 0 \ \ failed \\ < 0 \ \ elastic \end{cases}$$

    $$E_a = \nu_{ba} = \nu_{ab} = 0$$

  - Matrix failure mode in tension

    $$\sigma_{bb} > 0 \quad \text{then} \quad e_m^2 = (\tfrac{\sigma_{bb}}{Y_t})^2 + (\tfrac{\sigma_{ab}}{S_c})^2 - 1 \begin{cases} \geq 0 \ \ failed \\ < 0 \ \ elastic \end{cases}$$

    $$E_b = \nu_{ba} = 0 \rightarrow G_{ab} = 0$$

  - Matrix failure mode in compression

    $$\sigma_{bb} < 0 \quad \text{then} \quad e_d^2 = (\tfrac{\sigma_{bb}}{2S_c})^2 + \left[(\tfrac{Y_c}{2S_c})^2 - 1\right]\tfrac{\sigma_{bb}}{Y_c} + (\tfrac{\sigma_{ab}}{S_c})^2 - 1 \begin{cases} \geq 0 \ \ failed \\ < 0 \ \ elastic \end{cases}$$

    $$E_b = \nu_{ba} = \nu_{ab} = 0 \rightarrow G_{ab} = 0$$

    $X_c = 2Y_c$ for 50% fibre volume

- Tsai - Wu

  The equations that lead to failure prediction based on this criterion are the same ones that for the previous ones except for the tensile and compressive matrix mode:

$$e^2_{md} = (\frac{\sigma^2_{bb}}{Y_t Y_c}) + (\frac{\sigma_{ab}}{S_c})^2 + \frac{(Y_c - Y_t)\sigma bb}{Y_c Y_t} - 1 \begin{cases} \geq 0 \ \ failed \\ < 0 \ \ elastic \end{cases}$$

### Cohesive elements

Cohesive elements are also of interest in the development of the thesis. They are commonly used with the purpose of analysing delamination damage in composite materials. Cohesive acts as a joint, but instead of strain limit, the deformation is in terms of the relative displacements and due to the damage the size of the partition increases until it is removed. It is at this moment when both plies detach from each other and delamination appears. In order to explain how all the properties were found out in Section 3, first it is needed to explain the nature of the cohesive materials. They behave under mixed-mode traction separation and bilinear traction separation laws, shown in Figure 8 and 9. From this law, it can be expressed the energy release rates as they are the area of the triangle form by the peak traction and the ultimate displacement. This is applicable for both direction, normal and tangential, Equation 4 and 5.

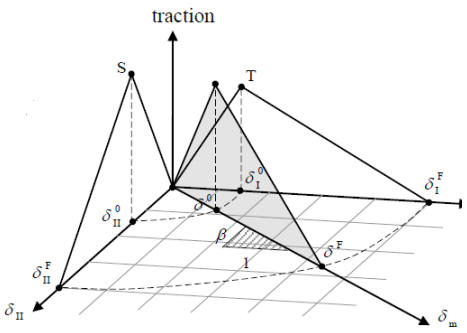


**Figure** 8: Mixed-mode traction separation law

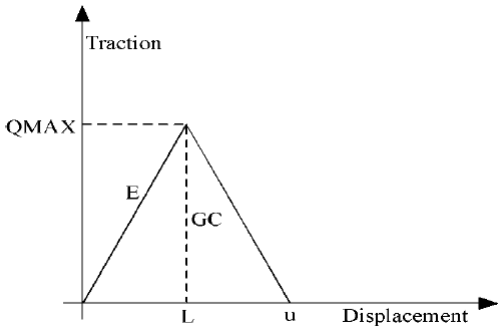


**Figure** 9: Bilinear traction-separation law

$$G_{Ic} = \frac{Tu_{ND}}{2} \tag{4}$$

$$G_{IIc} = \frac{Su_{TD}}{2} \tag{5}$$

The energy release rates as well as peak tractions in both directions were obtained from a paper [8]. With these properties and using equations 4 and 5, the ultimate displacements can be computed. And finally, to ensure that the peak is not past the failure point, the condition $\frac{u}{L}$ needs to be fulfilled leading to Equations

6 and 7.

$$\frac{u}{L} = \frac{2G_{Ic}}{E_N(\frac{T}{E_N})^2} > 1 \tag{6}$$

$$\frac{u}{L} = \frac{2G_{IIc}}{E_T(\frac{S}{E_T})^2} > 1 \tag{7}$$

### 2.2.3 Applications

Due to the properties mentioned in the previous sections, and as said in the introduction, composite materials in the aerospace field are becoming a main character. From the moment they started to appear around the 70s, the use of these materials in commercial aircrafts has increased up to a 50% in the case of the Boeing 787 and 53% in the Airbus 350XWB. In the following picture it can be observed how the growth of composite materials use has been exponential through these years.

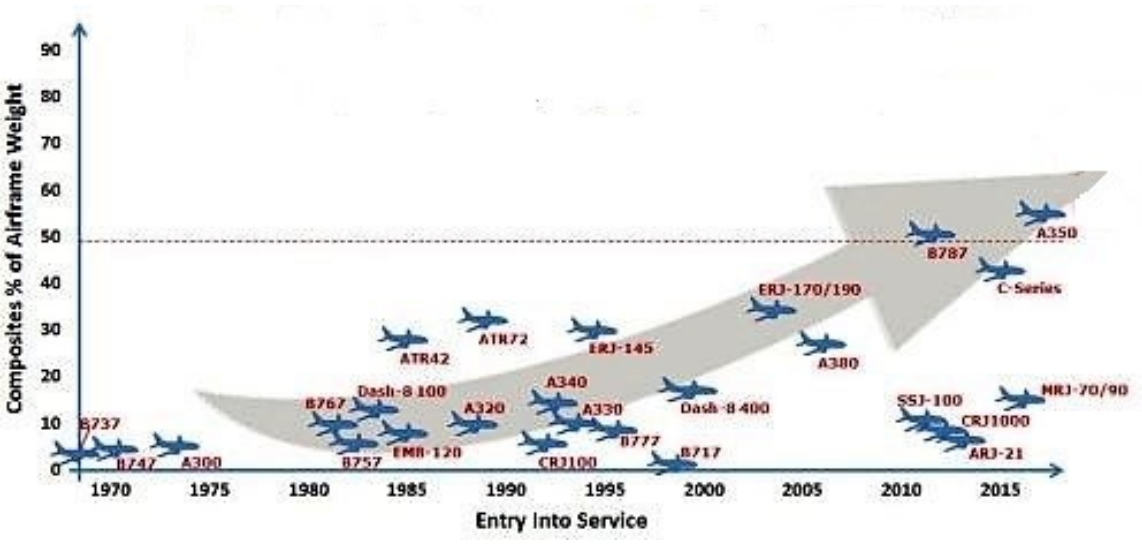


**Figure** 10: Used of composites along the years [9]

Regarding the different components of the aircraft in which composite has been implemented, one of the key factors are manufacturing processes of composite materials (Section 2.3). It has been necessary an improvement, for which purpose this thesis tends to help as well. In Figure 11 the introduction of different components by chronological order in Airbus aircrafts is represented.

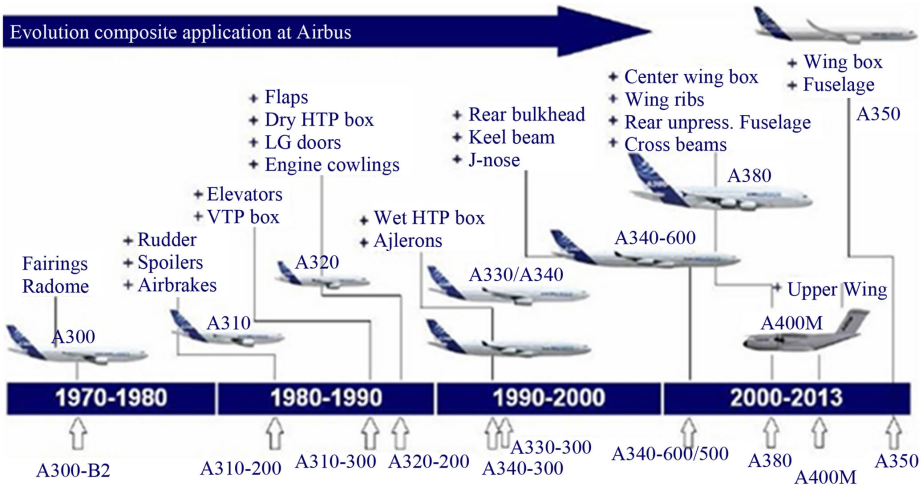


**Figure** 11: Components made of composite in Airbus [9]

Until this point, it has been only referred to civil aircraft. As always in this field, the latest technologies are first introduced in the military sector. More specifically, in the case of composite materials, development projects were born in the 70s in order to improve capabilities of fighter aircrafts, i.e., payload, agility, take-off and landing. The most typical example is the Eurofighter, with a 70% (surface area) of composite materials.


**Figure** 12: Eurofighter and its distribution of materials [2]

However, this is just a small overview of all the possible applications in the aerospace industry. There are many other situations in which these materials have been or can be used. For example, it should be mentioned that helicopters implemented composite rotor blades 40 years ago and nowadays all of them use this material. The space sector also tends to increase the use of composite in satellites, antennas,spacecraft structure...

Finally, composite materials are very important in many other fields such as biomedical industry, automotive industry (competition) or naval industry, so this thesis has an impact also in other sectors.

## 2.3 Manufacturing processes

The steps through which raw materials are transformed into the final products are named manufacturing processes. They include from the creation of the material to the different modifications until reaching the final part. Some important manufacturing processes are treating (such as heat treating or coating), casting, forming and machining.

The change from metallic to composite construction has naturally induced new methods in the design methodology of aircraft components. It has to be taken into account that not only the mechanical properties of composites differ from those of metals, but that a whole range of physical and chemical properties are different. Composite manufacturing processes are very complex due to all the parameters to be taken into account. Expensive raw materials, damage tolerance aspects, and the need for new inspection and repair philosophies need to be addressed. It is of special interest when referring to new materials design methods the following factors:

- Design simplification
- Low-cost processing
- Durability
- Maintainability

As the composite materials are a combination of the fibre and the matrix, due to complex shapes, and a lack of knowledge with respect to the behaviour when post-processing, one of the methods used is to give directly the shape when creating the material, before curing or hardening. This requires very complex machines. At the same time it avoids the problem of predicting possible damages after machining, drilling or milling, the most common methods in order to reach the final shape, although sometimes they cannot be avoided. When machining CFRP several problems may appear, like fibre-matrix delamination, fibre fragmentation and low surface quality. It is in this context, the difficulty of composite machining, where an orthogonal cut simulation to a CFRP becomes interesting to save expenses, learn to predict the behaviour and obtain more accurate failure criteria.

### 2.3.1 Machining

Machining is defined as a material-removal manufacturing process. By means of a cutting tool, part of the raw material is removed in a controlled way. Remaining material is usually known as chips. However, it has to be borne in mind that composite machining differs from the traditional ones, such as metal machining. The efficiency of this manufacturing process resides in the fact that the material is softer than the tool, so that a plastic deformation is performed in the part. In the case of composites, the election of the tool material is of crucial importance as, due to the high strength, the impact of the cutting edge tends to fracture the carbon fibres. Therefore, one of the most common problems is the abrasion and

rapid wear suffered by the tools. The most typical materials chosen to machine composite are carbide and diamond tooling.

A small introduction to the chips is also of importance. Chips are produced by the shearing process along the shear plane. Depending on the material and the velocity chips can be discontinuous or continuous. Discontinuous chips appear in hard and fragile materials cut at slow velocities. On the other hand, high cutting speed and ductile materials tend to produce continuous chips. This last option is to be avoided as it is very uncomfortable. In the case of CFRP the residual material is totally powdered.

- **Orthogonal cut**

  The reason why, between all the possible post manufacturing processes, it has been chosen an orthogonal cut, is explained by the fact that it simplifies the case while the results can be easily extrapolated to more complex processes, such as oblique cutting, as the angle of incidence does not normally exceed 15°. With this simplification, the interaction between the tool, the fibre and the matrix can be better understood.

  In the case of the orthogonal cut the tool is placed perpendicular to the machined sample while in the oblique one there is a certain angle.

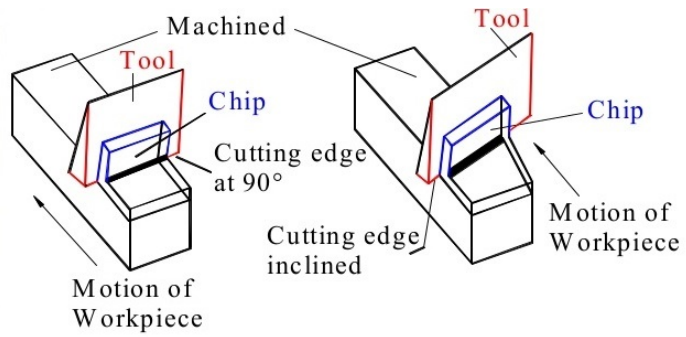


**Figure** 13: Orthogonal and oblique cut [10]

The advantages of the oblique cut with respect to the orthogonal one is that both milling and drilling, can be discretized as a sum of oblique cut operations. The inconvenient is that an oblique cut has three different force components instead of two, so the analysis become more complex.

In the following figure, the most relevant parameters of an orthogonal cut are shown and explained below.

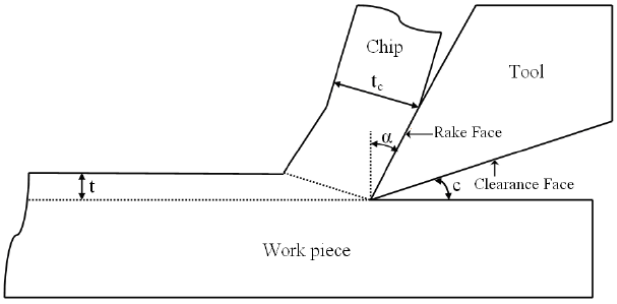


**Figure** 14: Orthogonal and oblique cut [11]

- Clearance angle (c): angle between the clearance face and the plane of the cutting velocity.
- Rake angle ($\alpha$): angle between the rake face and the normal plane to the cutting velocity.
- Chip thickness ($t_c$)
- Depth of cut (t)

If the clearance angle is very small, the contact between the sample part and the tool increases leading to higher temperatures and therefore, an earlier tool wear. On the other hand, if it is too big the cutting edge looses support.

The rake angle is directly related with the finish of the part. In case it is big, the tool will cut better reaching a good quality surface but leading to a faster tool wear.

Different speeds take action in the material removal process, the most important one is the cutting speed, lineal velocity between the tool and the sample. Another one is the velocity of the chips with respect to the tool.

Once the machining begins two main forces appear:

- Cutting force ($F_c$): it is measured in the horizontal direction. In this thesis is also named as principal force, it allows to know the required force to machine.
- Thrust force ($F_t$): force perpendicular to the direction of the cutting speed.

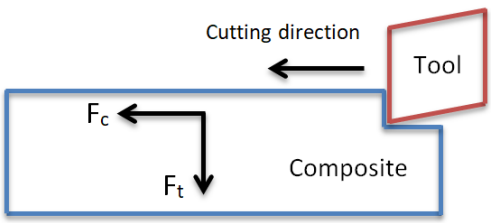


**Figure** 15: Forces direction

- **Drilling**

  It is one of the most common post manufacturing process done to composite parts, as many components of the aircraft need to be connected to others through holes. The orthogonal cut is used as a simplification of it. In Figure 16 it can be observed a scheme of a drilling and the similarity to the orthogonal cut.

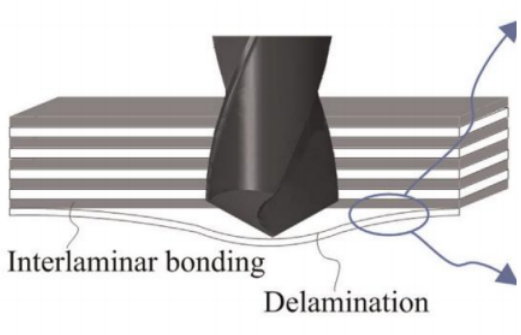


**Figure** 16: Drilling scheme and induced damage [12]

  However, the large forces of this machining process leads to internal delaminations, especially when the tool is drilling the last laminae. In the figure it is shown schematically what happens to the exit laminae.

## 2.4 Finite Element Method

Finite Element Method or FEM is a numerical method used to solve continuous problems by a discretization into simpler problems. It is used in engineer and mathematical physics, and as a result, nowadays it is possible to solve problems that could not be solved by traditional mathematical methods.

It decreases the time and the cost, reducing material waste and the time required for building prototypes, performing experiments and iterative improvements.

The method starts with the continuous problem and the set of equations that defines it. Then, the continuous solid is divided into a finite number of elements interconnected between them by nodes. Each of this element is also defined by the same set of equations that defines the global problem, therefore at the end of the discretization there will be N set of equations. On the nodes relies the fundamental unknowns, also named as degrees of freedom. They determine the state and/or position of the nodes. The differential equations are finally related with the value of the degrees of freedom. Finally there are N unknowns and N equations.

The problem is worked in matrix form due to the easiness of the computer to process data in this way.

Finally, a FEM software requires:

- Preprocessing: geometry, mesh, boundary conditions and properties are defined.
- Calculus: the program solves the N set of equations.
- Post-processing: results are graphically display.

### 2.4.1 Numerical models of composite materials manufacturing processes

FEM has been widely used in the case of composite materials simulations. This is due to the fact that the raw material is very expensive to be wasted in prototypes. It also helps to reach a better insight of the material, varying the boundary conditions as many times as required.

For this thesis the chosen software was LS-DYNA, as it offers many possibilities related with composite materials. The initial definition of the problem is done in ANSYS and then it is exported to include the properties of the materials in LS-PrePost. LS-PrePost is an advanced pre- and post-processor that is delivered with LS-DYNA. The user interface is designed to be both efficient and intuitive. It includes 3D plot animations and ASCII plotting.

Another software which is also very used for the same purposes is ABAQUS, however for the particular cases of composite materials and cutting process LS-DYNA is more powerful and uses a lower simulation time.

### 2.4.2 Post Processing data

After obtaining the results computed by the numerical software, the data has to be treated. In this case it is used Matlab, a mathematical software. The forces obtained include high fluctuations, therefore in order to get one magnitude some processing is required. It cannot be computed only the maximums and the minimums as some of the points obtained will not correspond to a real maximum but to one of the mentioned fluctuations. Therefore filters to obtain high and low envelope are used.

## 2.5 Experimental Approach

In the previous section it has been explained the numerical method used in the thesis and its advantages. However, in order for this model to be valid it has to, firstly, be compared with an experimental case and to check that the results are similar.

### 2.5.1 Instruments

This thesis takes another bachelor thesis as starting point: "Parametric study of the orthogonal cut machining in composite materials" by Gonzalo Raba and supervised by Víctor Criado. The author performed experimental orthogonal cuts

to the same composite sample considered in the thesis. The cutting force as well as the thrust force were measured for different cutting speed and depth of cut. The instruments used were an orthogonal cutting machine, and a dynamometer. During Section 4 there are constantly references to the experimental results.

Lastly, it was also used a high-speed camera in order to monitor the chip formation, a microscope to check delamination and a infrared thermographic camera to estimate the temperature field. The thermal analysis done in the experimental test is not included in this thesis.

### 2.5.2 Tool

The same tool is later defined in the software. The selected one, with its corresponding tool holder, is TCMW 16 T3 08 H13A. It is a carbide/cermet with a 7° clearance angle ($\alpha$) and 0° rake angle ($\gamma$). It was held by STGCR 1616H 16 tool holder. The cutting edge of this tool is not aggressive; it can be observed in Figure 17 that it forms a 90° angle.

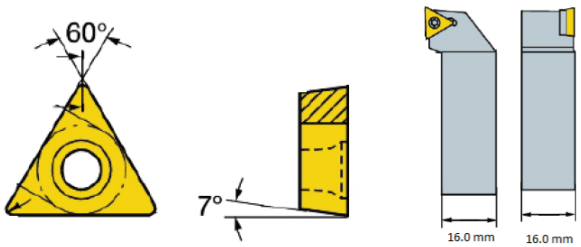


**Figure** 17: TCMW 16 T3 08 H13A scheme [12]

### 2.5.3 Tested material

The CFRP chosen was Carbon Epoxy IM7 MTM-45-1 which was made by a company called *Advanced Composite Group*. The material is a laminate made up of carbon fibre IM7 embedded in epoxy matrix MTM45. The laminated is composed of 24 plies oriented as $[(+45, -45, 90, 0)x3]_s$. The workpiece has an approximate thickness of 3 mm. The mechanical properties of the laminate were provided by the same company and are summarized in Table 3.

| Property | Value |
|---|---|
| $E_1$ (GPa) | 173 |
| $E_2$ (GPa) | 7.36 |
| $G_{12}$ (GPa) | 3.89 |
| $\nu_{12}$ | 0.33 |
| $X_t$ (MPa) | 2998 |
| $X_c$ (MPa) | 1414 |
| $Y_t$ (MPa) | 37 |
| $Y_c$ (MPa) | 169 |
| $S_{12}$ (MPa) | 120 |

**Table** 3: Mechanical properties

### 2.5.4 Cutting conditions

The experiment was performed under different conditions. These conditions were chosen following a certain criterion, CFRP cuts were though to be analysed under an industrial point of view.

| **Cutting speed [m/min]** | **Depth of cut [mm]** |
|---|---|
| 50 | 0.05 |
| 200 | 0.10 |
| - | 0.20 |

**Table** 4: Cutting conditions

# 3 Numerical model

In this chapter it is defined step by step the different parts of the model implemented in LS-DYNA and some other options tried before the validation. It has been sought a dependency relation between the different cutting parameters, thrust and cutting forces, geometry of the tool and orientation of the fibres. Therefore, the final aim of the model is to accurately represent the reality, but still keeps being simple, so these dependencies can be easily explained.

## 3.1 Geometry

Now it is described the main dimensions as well as the geometry variations due to the different depth of cut.

Firstly, in order to optimize the computational time, and taking advantage of the symmetric characteristics of the composite sample, it has been possible to set the model as symmetric. This means that only half of the sample has been defined in LS-DYNA, giving symmetric conditions with respect to the plane xy. The results obtained for the forces have to be later multiply by two, however the computational time saved is considerable. As a result, in Figure 18, it can be appreciated 12 out of the 24 plies. These plies are represented by the partitions done along the z axis, it is required in order to implement the different directions of each ply.

It can be also seen a smaller partition of 0.012m between the first and the second ply. It is required in order to implement the cohesive material. As said in Section 2 cohesive elements are used to study delamination damage and its function will be better explained when materials are described. However it is required to explain that in this numerical model it is only included one partition as cohesive elements increase considerably the computational cost. The location has been selected choosing the more likely places for delamination to occur. Therefore, this partition is very small, as cohesive elements only represent contact between the plies.

Partitions done along the y axis are explained in the mesh section (3.4) as they are done in order to optimize it.

Referring to the dimensions, they correspond with the ones from the experimental sample: 1.5mm of length (3mm considering the symmetry), 1 mm of width and 0.3 mm of height. In Figure 19, it can be observed the geometry of the tool, clearance angle is of 7°, while the rake angle is of 0° as the one of the tool described before. Depending on the depth of cut selected, the geometry varies as the tool is place above or below. The figures in this section show the geometry when d=0.1 mm.

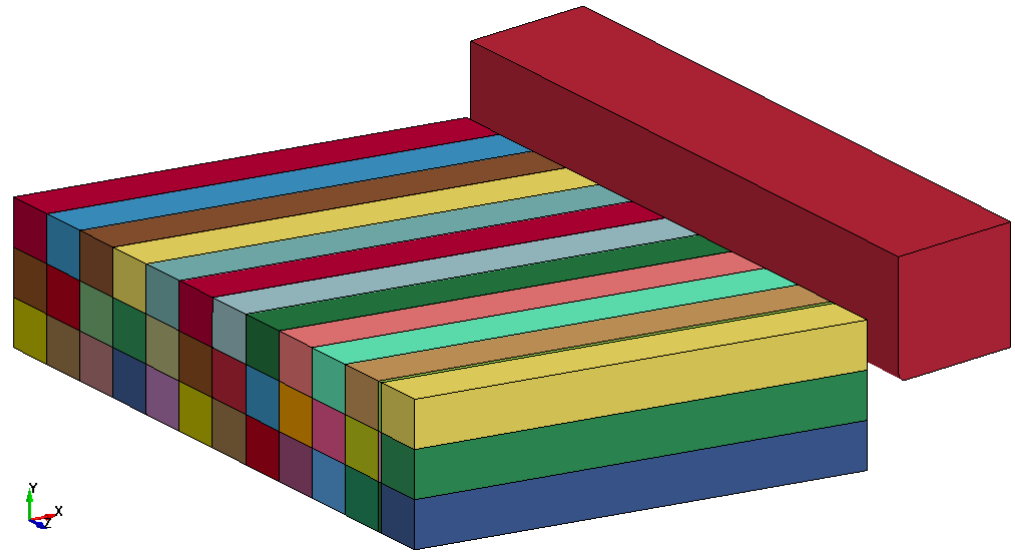

**Figure** 18: Isometric view

**Figure** 19: Left profile

## 3.2 Model characteristics

There are some settings define in the model which are not as visible as the geometry or the mesh, although they are of the same importance. The variables of control, the data recorded (named as database) and the contact between the different parts belong to these ones. Actually, it is in this section where more parameters appear.

### 3.2.1 Control

In the software it was defined 7 different control variables among many others: bulk viscosity, contact, energy, hourglass, solid, termination and timestep.

- Bulk viscosity: in LS-DYNA bulk viscosity is essential to treat shocks, otherwise it can lead to instabilities when solving. It is set to the default values.

- Contact: here it can be changed the default for computation with contact surfaces. Some variations were made with respect to the default values.
- Energy: provides controls for energy dissipation options. Some modifications were also done.
- Hourglass: it modifies a viscosity coefficient used in finite element analysis. It was also varied.
- Solid: the parameters defined here affects the solid element response.
- Termination: it indicates when to stop the simulations by a termination time or termination cycle, for example.
- Timestep: in this control it can be modified the structural time step size. The parameters chosen considerably affect the computational time, the memory required and the precision of the results.

### 3.2.2 Contact

The contact types between the different parts is assigned with these cards. Moreover, by default the software there is no contact between the composite plies, they act as the same solid part.

In order to create a contact between the whole composite part including the cohesive element, automatic surface to surface contact is defined. It is set for slave the cohesive parts (Figure 21) and for master part the composite one (Figure 20). This way errors when the whole cuboid interacts with the tool are avoided.

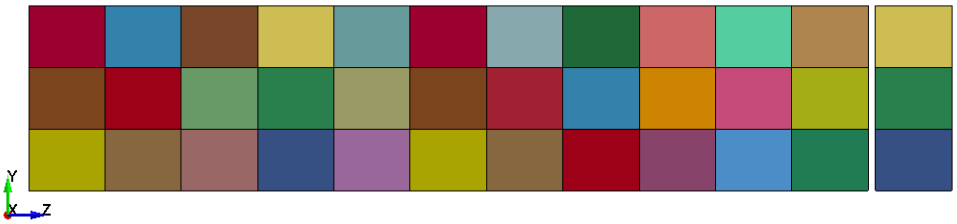


**Figure** 20: Master parts for contact 1

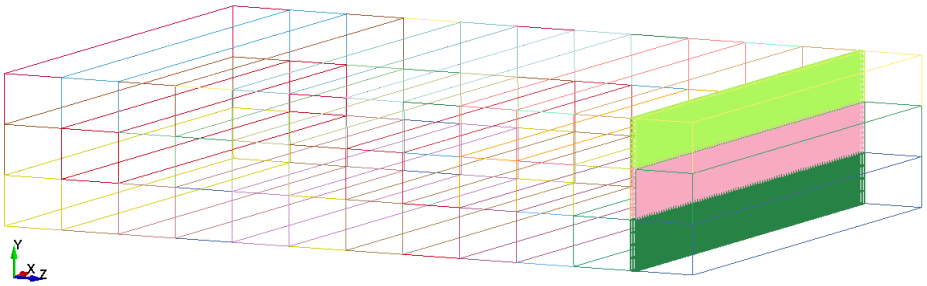


**Figure** 21: Slave parts for contact 1

The contact designated between the tool and the composite sample is eroding nodes to surface contact. In this case the slave part is the composite (Figure 23), as it is the one who suffers damage, while the master part is the tool (Figure 22). This assignment is done considering the hardnesses of the materials and which part damages the other one. It is considered a static and dynamic coefficient of friction of 0.3 and 0.1, respectively.

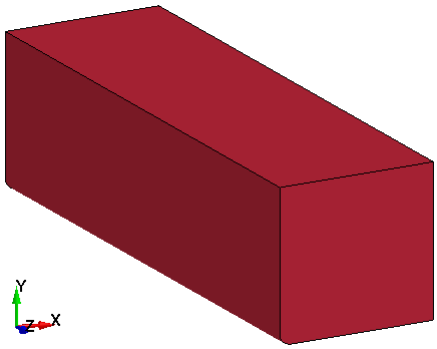


**Figure** 22: Master part for contact 2

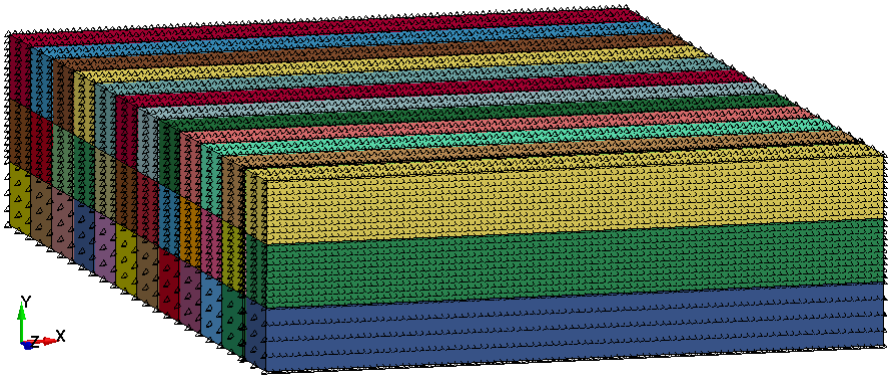


**Figure** 23: Slave parts for contact 2

### 3.2.3 Database

Three different cards were defined in this section: ASCII option, binary D3plot and binary RUNRSF.

- ASCII files include the element data, global data, different nodal forces and the most important one for the purpose of the thesis, resultant interface forces. The data is extracted with matrix form, although the software also shows it graphically. Resultant interface forces are computed for the different contacts defined, and from the point of view of the slave part and the master part.

- Binary D3plot contains information to plot the 3D simulation of the cutting. In this case this information is the interval of time between the outputs.

- RUNRSF specifies the time to restart a file in the same cycle. It affects the memory required for the computation.

## 3.3 Boundary conditions

Three different boundary conditions are defined: constant velocity of the tool, fixed support and z-displacement constrained in the symmetry plane.

The tool surface located opposite to the composite material (yellow surface in Figure 24 is defined with an x velocity component. It varies depending on the simulation between 1, 50 an 200 mm/min. The velocity is constant and lineal and it makes the tool move and cut the composite sample.

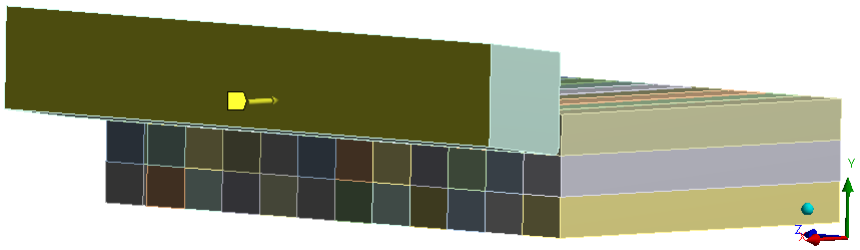

**Figure** 24: Velocity scheme

Due to the symmetry explained in the geometry section, during the whole simulation the displacement in the z axis is constrained for those surfaces placed at the symmetry plane. Surfaces can be appreciated as the yellow ones in Figure 25. The restrictions included can be seen in Table 3.3.

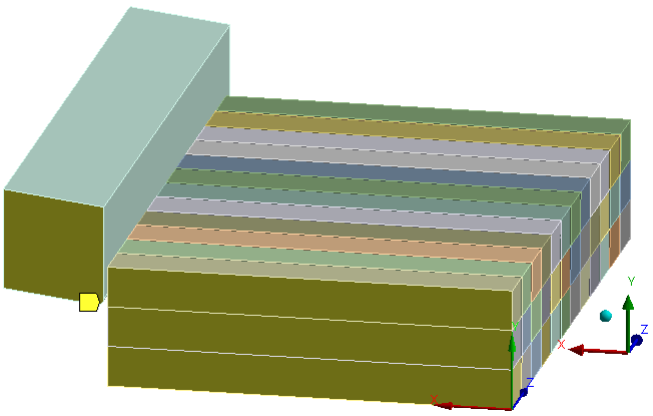

| **Z-contrains** |
|---|
| $u_z = 0$ |
| $M_x = 0$ |
| $M_y = 0$ |

**Figure** 25: Scheme of surfaces constrained in the z-axis

Finally, a fixed support which represents the support in the experiment is defined. It means that it absorbs horizontal and vertical forces as well as moment. The fixed support is assigned to the blue surfaces shown in Figure 26 for a depth cut of 0.1mm, only two partitions along the y axis as the third one is the material cut. The composite surfaces limited by the same partitions opposite to the symmetry yz plane cannot be seen in the Figure but they are also included. The fixed

support surfaces vary as a function of the depth of cut, so that the free composite corresponds to the cut material.

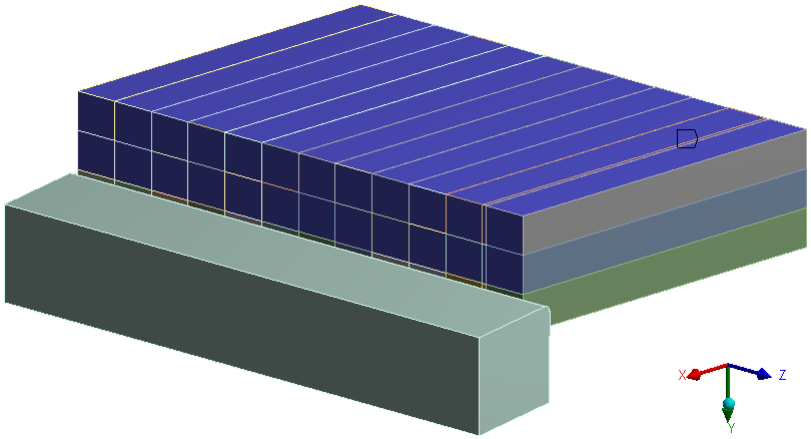

**Figure** 26: Fixed support scheme

## 3.4 Mesh

This is one of the most important parts of the model as it directly influences the results. An incorrect mesh can lead to a lack of accuracy. Due to this a sensitivity analysis is performed. At this point the final elections to define the mesh are shown and justified. Mesh varies depending on the depth of the cut performs. In the following figures (27 and 28) the mesh done for the simulation in which the depth is of 0.1mm can be appreciated. It is explained below and after all the differences with the other two models are also shown.

First of all, as the composite sample is a cuboid, it is possible to select a structured mesh for it. This means that the mesh is composed of brick elements in 3D, what implies many advantages when solving numerically, as the (i,j,k) leads to more efficients loops. This options is not possible in the xy plane of the tool due to its shape.

In the zy (Figure 27) plane the divisions has been made by setting a number of divisions per ply. After performing the sensitivity study, considering time and accuracy, the final number of divisions is 2. In this case it is the same number of divisions for the whole part.There is only an exception and it is the cohesive ply, it is meshed as one and only element. The reason is that when diving it in more elements some errors appear in the model due to its particular properties (it is eliminated when it reaches a certain displacement).

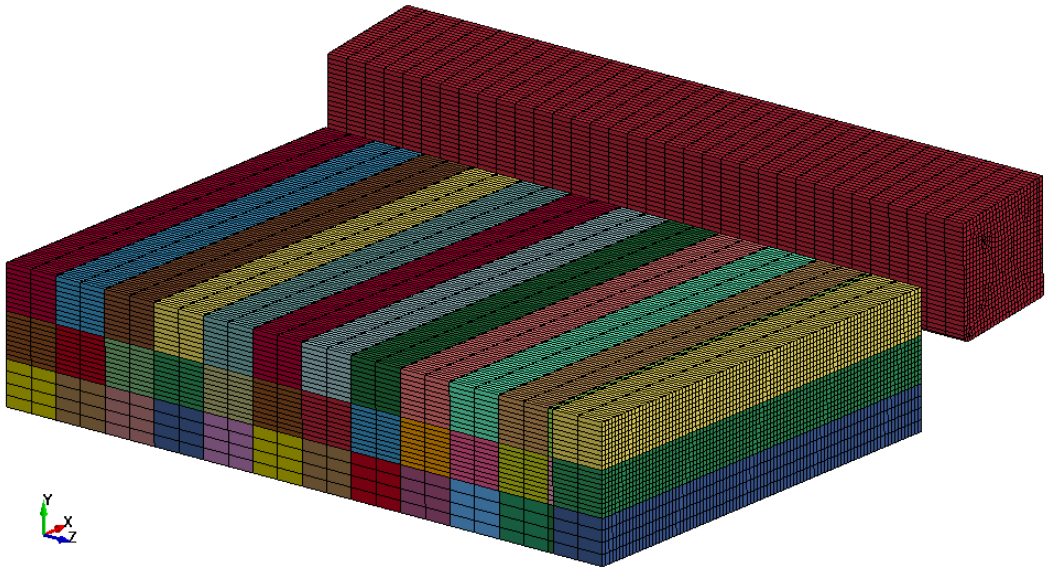

**Figure** 27: Isometric view of the mesh

In the xy plane (Figure 28) two different mesh sizes can be identified, one relatively fine and one relatively coarse. The elements of the first one are of the order of $10^{-5}m$, while the elements of the second one are of the order of $10^{-4}m$. As it was said previously, there is a explanation of the three partitions done in the plane xy related to the mesh. The finer the mesh is, the more accurate the results obtained are. However, it also adds an extra computational time. For this reason, in the composite, it has been set a fine mesh in the two partitions aside the cutting plane, while the third one can be considered as a relatively coarse mesh. The results in this last partition are not as important as the other one. In the tool it can be found again a fine mesh, as a small size of the elements in the cutting edge is required in order to later appreciate the exact point where the abrasion appears. Due to the different depths of cut in Figure 29 and 30, it can be seen that a different mesh is done, to be as close as possible to the cutting plane and optimize the computational time.

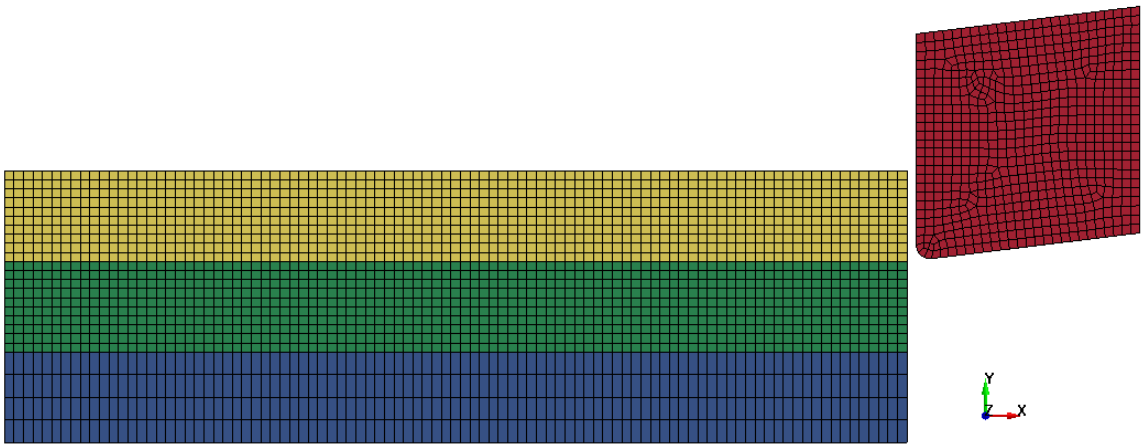

**Figure** 28: Left profile showing the mesh

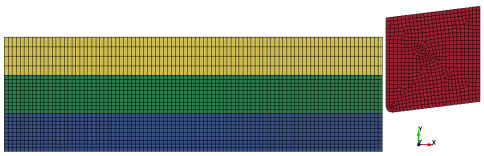

**Figure** 29: Mesh for d=0.2mm

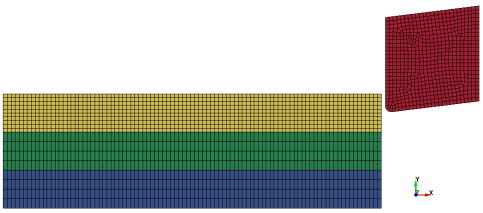

**Figure** 30: Mesh for d=0.05mm

### 3.4.1 Mesh sensitivity analysis

Before the sizes for the mesh were selected it was done a sensitivity analysis. It consists in varying the mesh until the changes between the final results are stabilized. The case selected for the study was v=200 m/min and d=0.1mm. As the forces affect mainly the part defined with fine mesh, only the dimensions of this one were varied. 5 different meshes were considered, Table 5 shows the dimensions selected.

| | Mesh 1 | Mesh 2 | Mesh 3 | Mesh 4 | Mesh 5 |
|---|---|---|---|---|---|
| Fine size [m] | $2.5\ 10^{-5}$ | $1.5\ 10^{-5}$ | $1.2\ 10^{-5}$ | $1\ 10^{-5}$ | $8\ 10^{-6}$ |

**Table** 5: Mesh dimensions

In the following graph it can be appreciated the numerical force computed in the different cases. As it can be observed, for the cases in which the mesh is bigger the fluctuations are more significant until the force stabilizes. In the case Mesh 1 it even reached an error and the simulation stopped due to the instabilities in the element. The election of the mesh is the crucial importance so that the results are reliable.

It is observed that the difference in the time that it takes to stabilize between cases Mesh 3, Mesh 4 and Mesh 5 is almost negligible. However in this case there exists a big difference in the computational time, what explains that the time computed in the case Mesh 5 is shorter. From this point a compromise was required and the selected mesh was the one from the case Mesh 4.

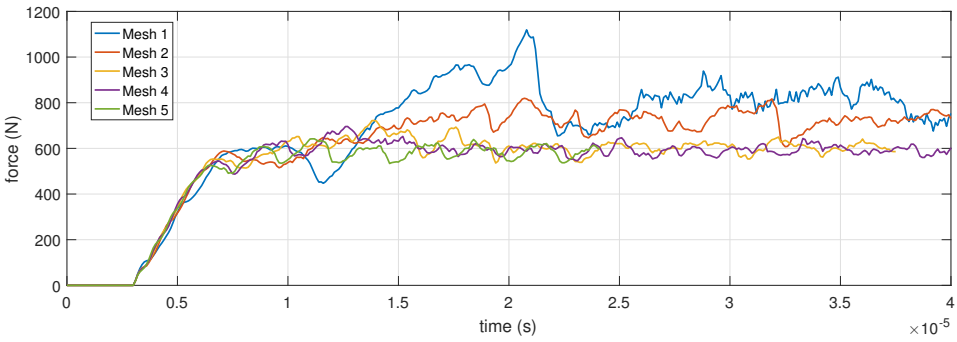


**Figure** 31: Principal force, v=200m/min d=0.1mm

## 3.5 Material

The different final materials, as well as some trials, are explained below, with the corresponding properties and how they have been obtained when it is considered of interest for this thesis.

### Tool

The main objective of the material defined for the tool is that it is sufficiently hard to not get deformed when cutting the composite sample. Therefore an elastic material has been chosen. Although it does not behave as the real tool because the properties are not provided, it is still possible to appreciate whether the maximum wear appears. Properties of carbide have been used, shown in Table 6.

| |
|---|
| $\rho = 156000\ kg/m^3$ |
| $E = 650\ GPa$ |
| $\nu = 0.22$ |

**Table** 6: Carbide properties

### Composite

There are different card options to define composite materials in LS-DYNA. The main restriction in this thesis is the fact that the model is defined as solid (not shell) so some of cards are directly discarded.

Three different materials were tried during the different models:

- Material 022: the most basic composite was implemented, named as Composite Damage. It follows the failure criteria proposed by Chang-Chang. In order to define it the following properties are required: $\rho$, $E_a$, $E_b$, $E_c$, $\nu_{ba}$, $\nu_{ca}$, $\nu_{cb}$, $G_{ab}$, $G_{bc}$, $G_{ca}$, and bulk modulus. Then, in order to calculate when failure occurs additional information is needed: $X_T$, $Y_T$, $Y_C$, $S_N$, $S_{YZ}$ and $S_ZX$. However, the forces reached with this material did not achieve an order of magnitude similar to the experimental measurements.

- Material 054/055: it is named Enhanced Composite Damage, and as it can be deduced it is an improved version of the previous one. In this case the failure criteria between Chang-Chang and Tsai and Wu can be selected, being the first option the one that was selected for the models launched with this material card. The performance and measurements of failure under compression are refined, what is convenient for the case of orthogonal cutting. In this case the properties defined are the same ones that in the previous material 022 except for the bulk modulus, which is not used. To calculate failure, in addition to $X_T$, $Y_T$, $Y_C$, $S_C$, maximum strain for fibre under compression and tension are also included. After launching several cases varying some of the possible parameters, the previous problem persists, the principal force varies among 70-90 N, very far from the

experimental measurements. Some explanations can be associated to two different aspects. First, in scientific papers these two materials were used to simulate instantaneous impacts but not a continuous forces such as the one in the orthogonal cut. Secondly, this model does not include a thermal analysis, which is of considerable importance, although out of the scope of this thesis.

- Material 02: a basic card was finally chosen, named Orthotropic elastic material. This is the most simple and general way of defining an orthotropic material. Through this card, the properties of the material ($\rho$, $E_a$, $E_b$, $E_c$, $\nu_{ba}$, $\nu_{ca}$, $\nu_{cb}$, $G_{ab}$, $G_{bc}$, $G_{ca}$) are set, but the failure criteria have to be separately implemented. Therefore, after defining the properties in the specified directions an extra card provides failure criteria. This card is named add erosion, it includes many failure criteria that act independently, and once one of them is fulfilled the element is removed. The criterion used in this case is maximum effective strain at failure. This parameter, together with cohesive properties, is the one varied to validate the model.

| | $\rho$ $[kg/m^3]$ | $E_a$ $[GPa]$ | $E_b$ $[GPa]$ | $E_c$ $[GPa]$ |
|---|---|---|---|---|
| Material 02 | 1600 | 173 | 7.3 | 7.3 |

| | $\nu_{ba}$ [-] | $\nu_{ca}$ [-] | $\nu_{cb}$ [-] | $G_{ab}$ $[GPa]$ | $G_{bc}$ $[GPa]$ | $G_{ca}$ $[GPa]$ |
|---|---|---|---|---|---|---|
| Material 02 | 0.014 | 0.017 | 0.330 | 3.89 | 3 | 3.89 |

**Table** 7: Composite properties

It is also remarkable how the directions of the different plies are implemented. At the beginning of the thesis composite materials were calculated for each direction. Nevertheless, after researching, the possibility to implement the direction in the solid parts was found out so that by defining the 0° properties, and in case that the card considers orthotropic behaviour, the software computes the properties for the different directions. In Figure 32 the directions can be appreciated, red vector indicates the principal direction while green vector the normal direction. As the tool is isotropic it is not necessary to define its directions and it is not included in the Figure.

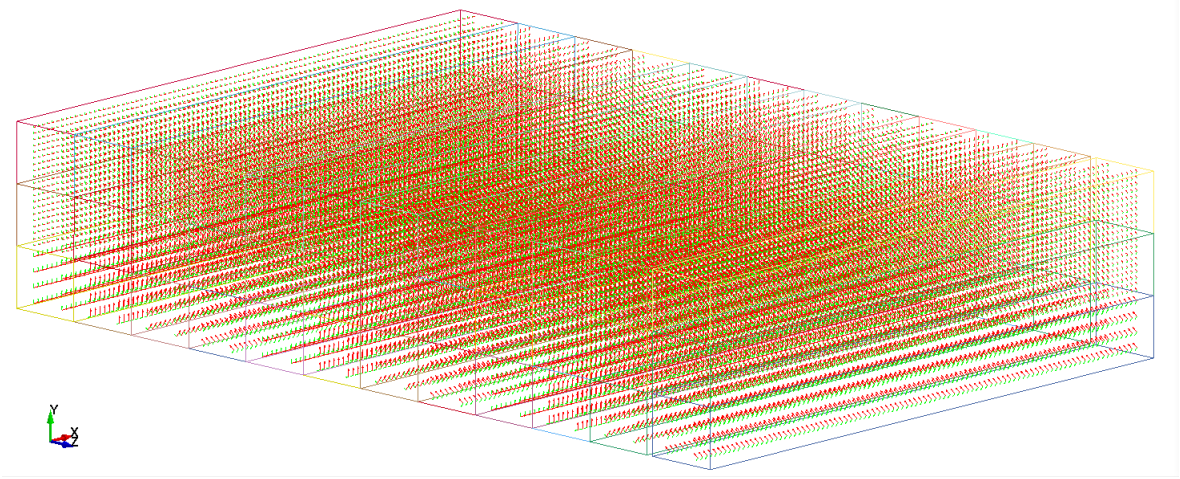

**Figure** 32: Composite directions in the 3D model

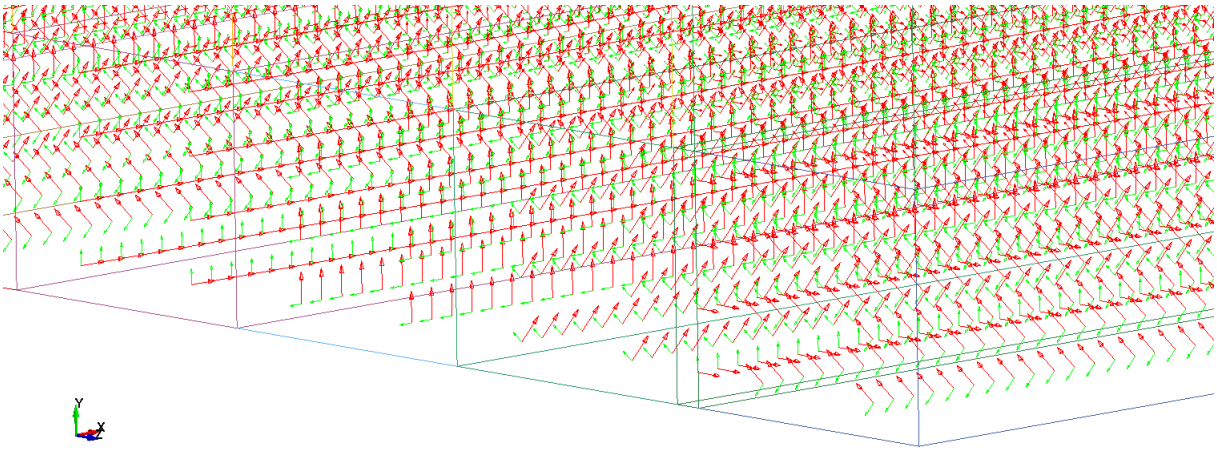

**Figure** 33: Zoom of the composite directions in the 3D model

### Cohesive

One of the main purposess of this numerical model is to analyse the delamination of the part. To this end, a small partition between two plies was implemented and defined as cohesive material. Also, the implementation of the cohesive contributes to reach a more accurate value of the force, as it acts as a parameter to modify it, although less directly than the strain limits.

In LS-DYNA there exists four different cohesive materials in which the parameters and conditions given differ. For this case it has been chosen MAT_138, named cohesive mixed mode.

Finally, the properties defined in the LS-DYNA card were obtained based in the cohesive used in the paper [8], because of the similarity in the materials, and

using the equations explained in Section 2. In Figure 34 it can be seen the width of the cohesive elements in-between the plies.

| $G_{Ic}$ [N/mm] | $G_{IIc}$ [N/mm] | $\sigma_{uI}$ [MPa] | $\sigma_{uII} = \sigma_{uIII}$ $[MPa]$ |
|---|---|---|---|
| 0.306 | 0.632 | 40 | 40 |

| $u_{ND}$ $[mm]$ | $u_{TD}$ $[mm]$ | $E_N$ $[GPa/m]$ | $E_T$ $[GPa/m]$ |
|---|---|---|---|
| 0.0153 | 0.0317 | 27000 | 13000 |

**Table** 8: Cohesive properties

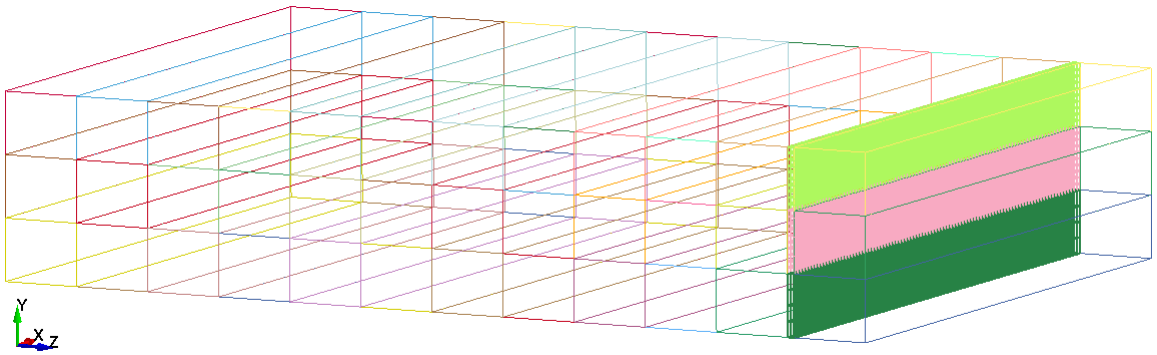


**Figure** 34: Cohesive elements

# 4 Results

This section is divided in different parts. First, the method followed in order to validate the model is explained, showing the different choices and justifying the selected ones. Secondly, the model is proved for different cutting conditions. A comparison of the experimental thrust force and the numerical one is done. Hereafter, delamination is studied in the cohesive elements as well as the tool damage. The last part corresponds to a mesh sensitivity analysis, so that the influence of the mesh in the model can be studied. During the whole section there are constantly references to the thesis mentioned before, "Parametric study of the orthogonal cut machining in composite materials" by Gonzalo Raba.

## 4.1 Validation

With the purpose of validating the model, one of the different cutting conditions has been selected. Due to the time that it takes the software to reach a stable result the highest velocity, v=200 m/min, has been selected as it is faster computed. On the other hand, a depth cut of 0.1mm has been chosen. As explained before, the numerical model is validated with respect to an experimental test, the principal force measurement of the test with the same cutting condition can be shown in Figure 35 and 36. The principal force is the selected one as it is the most important force involved in the process.

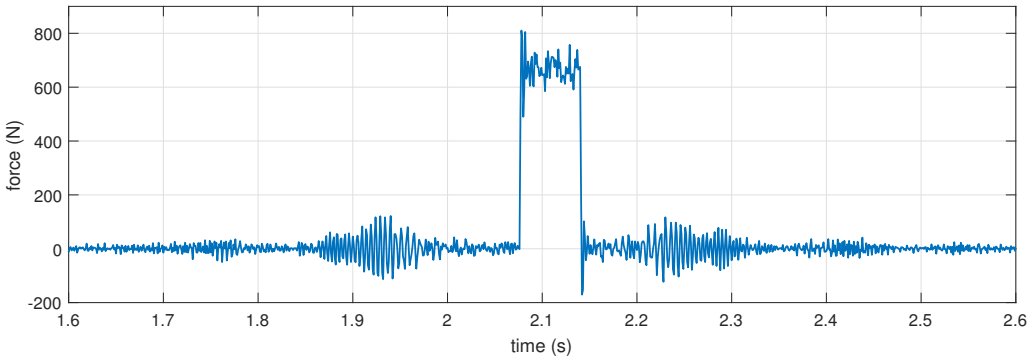


**Figure** 35: Principal experimental force, d=0.1 v=200m/min

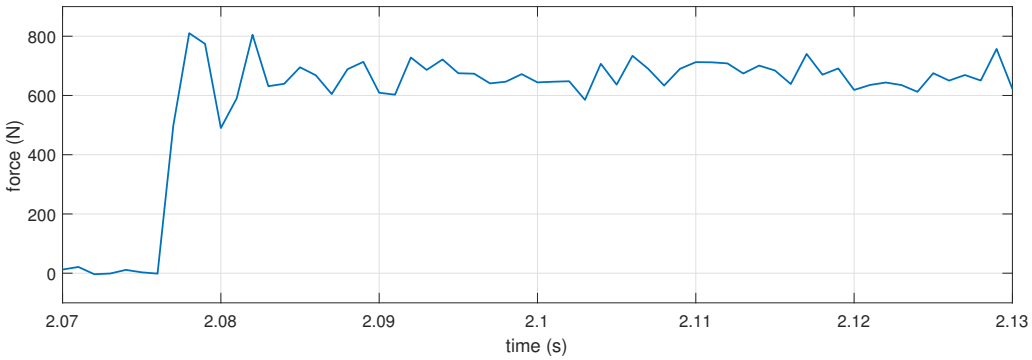


**Figure** 36: Principal experimental force zoom, d=0.1 v=200m/min

Many different models were launched and compared with the experimental results, the main variation among these models is the value of the strain limit explained in Section 3.5. Finally two models were selected, Model 1 is set with a stain limit of 2, while a value of 1.5 was depicted for Model 2. It can be observed in Figure 37 that, as expected, Model 1 requires a higher principal force in order to cut the CFRP. The 0.5-strain-limit difference corresponds to approximately 60 N in the numerical model. It can also be observed that at the beginning the fluctuations are larger and then it tends to stabilize. This is a normal behaviour as the first part corresponds to the moment when the tool touches the composite workpiece and then it starts cutting the sample.

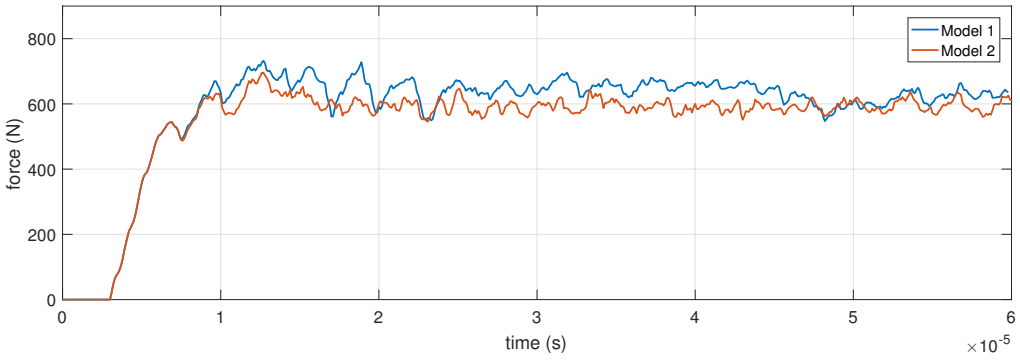


**Figure** 37: Comparison of different strain limits, d=0.1 v=200m/min

Comparing Figure 36 and 37 it can be observed that in the numerical force the measurements are taken within smaller increments of time, this is not possible in the case of the experimental force as they depend on the instruments used. Moreover, a relevant difference is that in the experimental results the force starts directly at its highest magnitude while in the numerical results at the beginning the force is increasing slowly, this can also be attributed to the difference in the increments of time used for measuring.

Although in Figure 35 it can be observed that the cut lasts less than 0.1s, in the figure above the order of the time magnitude is $10^{-5}$ s. This is because the simulation is ended once the results were stable due to the high computational cost. To let the reader guess the amount of the sample cut up to that time, it is included Figure 38. However the required time to reach this point varies among Model 1 and 2.

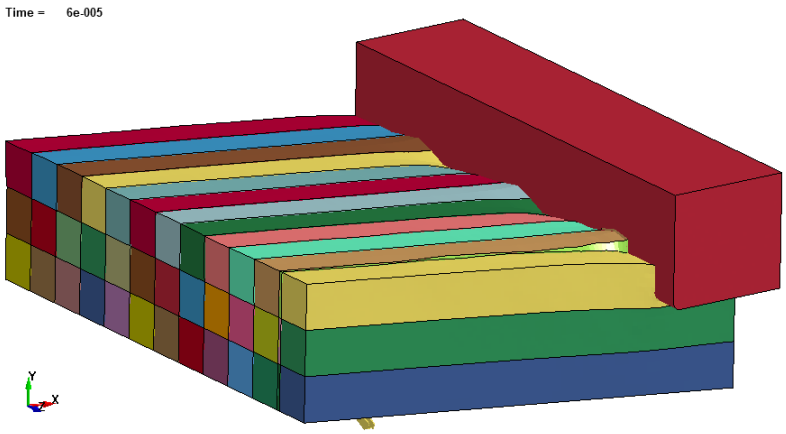


**Figure** 38: 3D model at t=6 $10^{-5}$

As it has been explained, these are the forces computed by the software among the whole cutting process. In order to compare only one magnitude a postprocessing is required. In Figures 39 and 40 it can be observed the high and low envelopes of the signal computed with Matlab. It must be mentioned that for calculating the average principal force the maximums of the high envelope are only considered. The reason is that the low envelope corresponds to moments in which elements of the model are eliminated and therefore the force is suddenly reduced until the tool reaches the next element. This can be improved with a finer mesh for which it takes less time to the tool. However, in this thesis it is chosen to consider the high envelope in order to compute the average force. So, once the high envelope is obtained, the maximums are computed through a simple code and the mean is obtained.

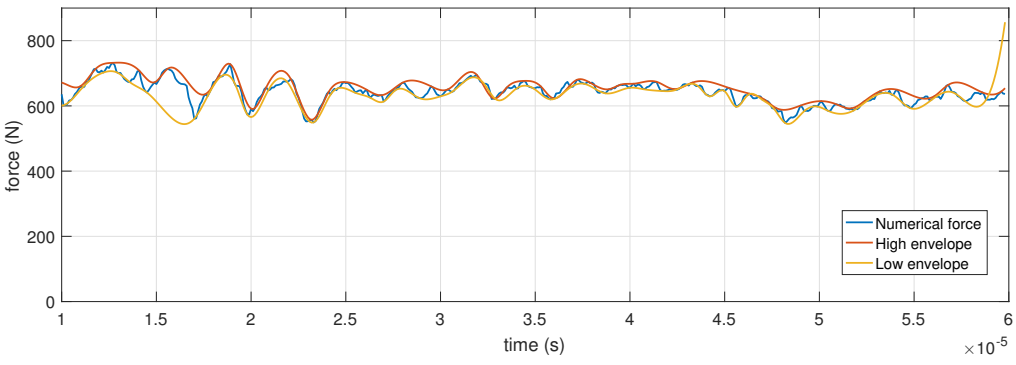


**Figure** 39: Model 1 principal force, d=0.1 v=200m/min

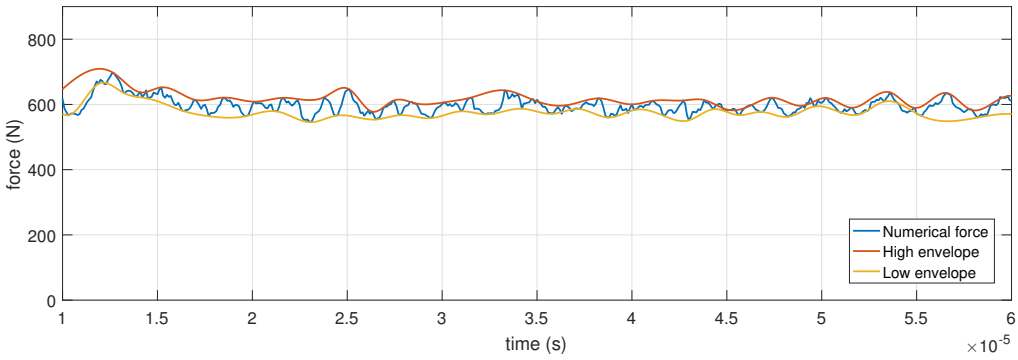


**Figure** 40: Model 2 principal force, d=0.1 v=200m/min

After the postprocessing, the results obtained, as well as the corresponding experimental force, are shown in Table 9. It can be observed that the closest numerical model to the experimental one is Model 1. However, it can be observed that in both cases the error is less than 15%, what can be considered accurate enough for the numerical model. It is at this point when the computational time becomes a determinant factor. An overview of the difference in computational time is given, for reaching the same simulation time (t=9.610⁻6) Model 1 takes 1 hour and 35 minutes while Model 2 takes 50 minutes. Therefore, considering the error and the computational time, it was decided to select Model 2 for the rest of the cases analysed in this thesis. Although the model can always be improved, the time is always a key factor as it affects directly the economical aspect.

| | Experimental | Model 1 | Model 2 |
|---|---|---|---|
| Principal force [N] | 707.36 | 684.36 | 632.93 |
| Error [-] | | 3.25% | 10.52% |

**Table** 9: Comparison of principal forces

Once it is decided to keep working with the strain limit of 1.5, the same model is launched for a different cutting velocity, v = 50m/min, in order to check if the tendency followed by the force in the experimental test occurs in the numerical model. This is another form of validating the model, not only the principal force must be similar but the variation with respect the velocity must be the same. In Figure 41 and 42, the experimental principal force is shown, while Figure 43 shows the numerical principal force with the corresponding envelopes.

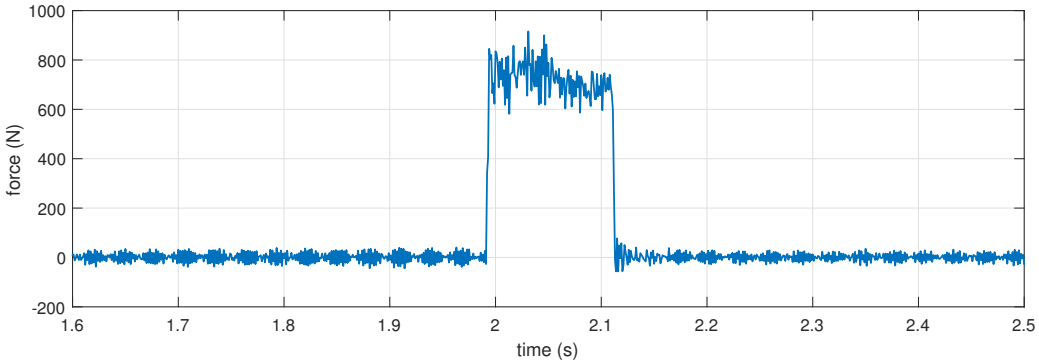


**Figure** 41: Principal experimental force, d=0.1 v=50m/min

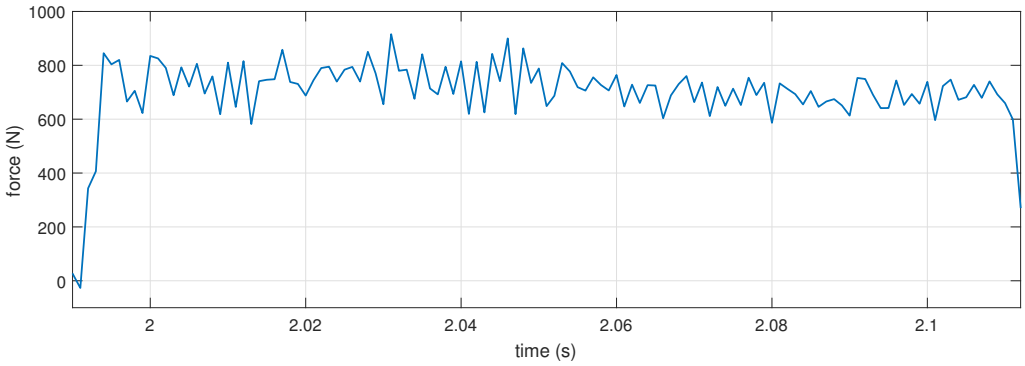


**Figure** 42: Principal experimental force, d=0.1 v=50m/min

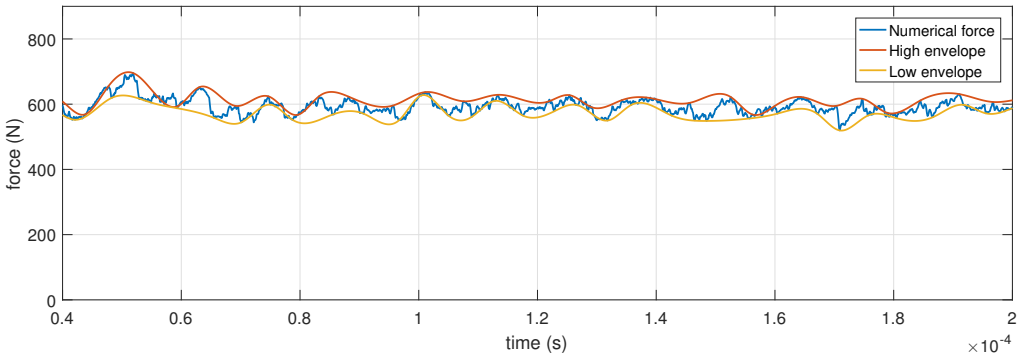


**Figure** 43: Principal numerical force, d=0.1 v=50m/min

The same process as before has been followed in order to get a magnitude for the principal force, which can be appreciated in Table 10. In the same table the principal force is compared with the experimental one for the three velocities. When the velocity is decreased the principal force is also lower, and this occurs

in both cases, the experimental and the numerical model. Therefore, it can be considered that the model for this depth of cut is validated.

| | Experimental principal force [N] | Numerical principal force [N] |
|---|---|---|
| v = 200 mm/min | 707.36 | 632.93 |
| v = 50 mm/min | 674.88 | 616.99 |

**Table** 10: Comparison of principal forces at different velocities

## 4.2 Results

### 4.2.1 Force

**Principal force at different cutting conditions**

With the validated model now different cases are launched and principal force is analysed. The only variations are done in the geometry and the mesh, the rest of parameters are maintained.

First the principal force obtained when varying the depth cut is shown in Figure 44. As it can be observed the software computes the force directly proportional to the surface. Therefore when the depth cut is reduced to the half the force is decreased as well. the same process as before is followed in order to get a magnitude, and the results can be observed in Table 11 In the experimental test, the force also varies with the same tendency but in the order of 30-40 N, so the force is still close to 700 N. Therefore it can be said that the model is not valid for different depth of cut, as the principal force cannot be computed from it.

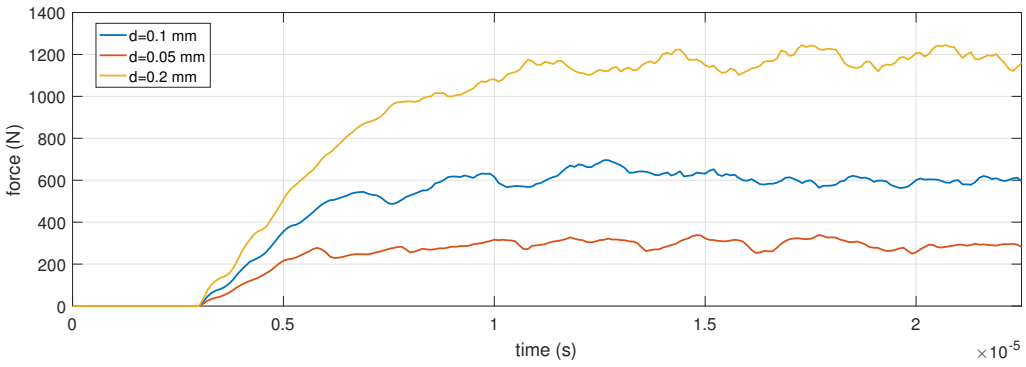


**Figure** 44: Principal force, v=200m/min

However, the tendency of the model with respect to different velocities can still be studied. In the table below the results for all the cutting conditions compared with the experimental ones are shown, after launching six different cases. Graphs are not been shown as the same procedure than before is followed in order to compute the force magnitude.

It is observed that, in all the cases the principal force is lower when the velocity decreases. Therefore, with respect to the velocity variations, the model is still valid.

| | Experimental principal force [N] | | Numerical principal force [N] | |
|---|---|---|---|---|
| | v=200m/min | v=50m/min | v=200m/min | v=50m/min |
| d = 0.05 mm | 643.24 | 631.86 | 343.08 | 330.51 |
| d = 0.1 mm | 707.36 | 674.88 | 632.93 | 616.99 |
| d = 0.2 mm | 736.28 | 725.57 | 1344.92 | 1208.76 |

**Table** 11: Principal force for different cutting conditions

**Thrust force**

Although it is not considered in order to validate the model, as it is not as important as the principal force, the results of the thrust force obtained in the numerical model and the experimental test are compared. The case selected is the one used to validate the numerical model: d=0.1, v=200m/min.

In Figure 45 the experimental thrust force is observed, which is of the order of 35N. The next figure shows the numerical results in which the force reaches a value around 550 N. Therefore it can be established that the model is not valid for computing the thrust force.

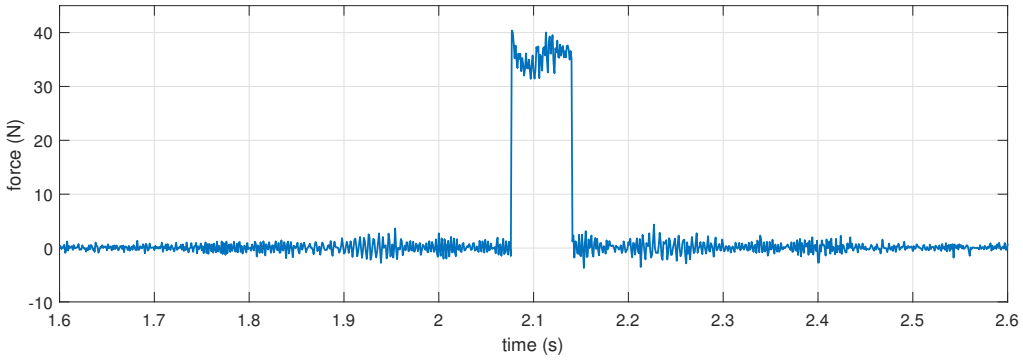


**Figure** 45: Experimental thrust force, v=200 m/min d=0.1 mm

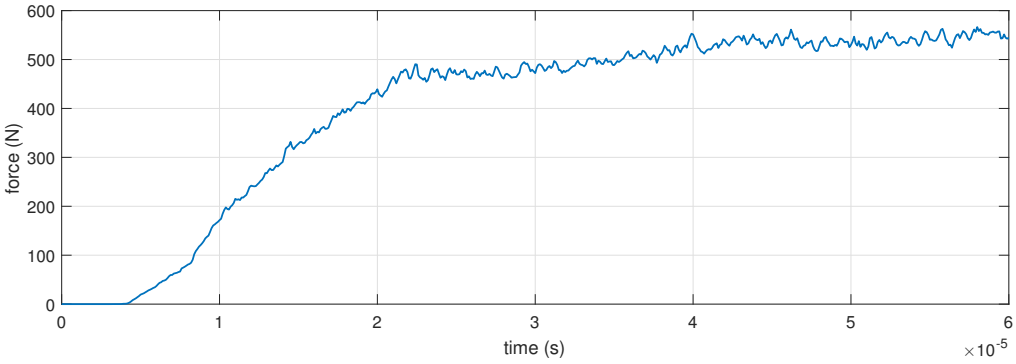


**Figure** 46: Numerical thrust force, v= 200 m/min d=0.1 mm

### 4.2.2 Stress

#### Von Mises stress

One of the main advantages of FEM is that it is possible to analyse in a visual way the state of the composite material at a certain time. In the following graphs it can be observed Von Mises stress for all the cases launched. The composite is cut up to the same point as the time selected has been computed as function of the two different velocities. In the figures it is possible to appreciate which of the laminates suffers the most and therefore, to determine the directions in which damage is higher. In the left part it can be observed the maximum and minimum values of the stress, however the maximum value corresponds to the tool and the legend has been adjusted in order to better appreciate the composite material.

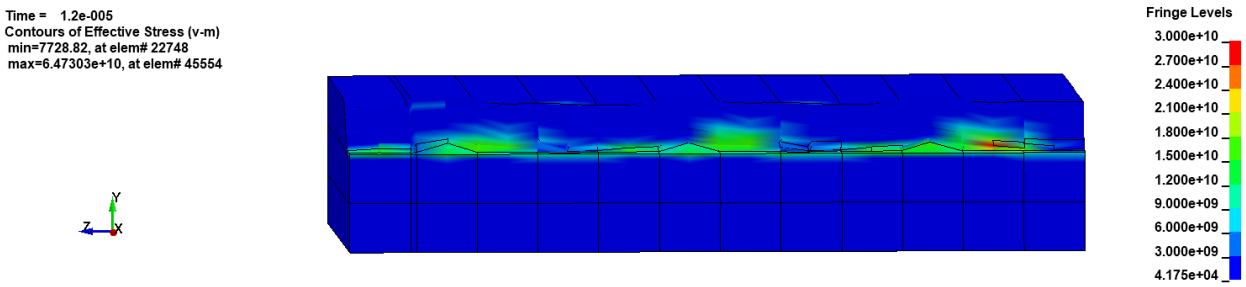


**Figure** 47: Von Mises stress [Pa], v=200m/min d=0.1mm

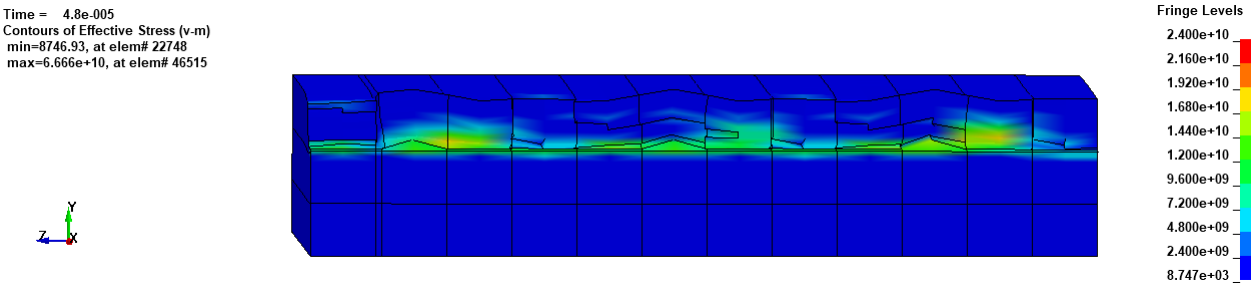


**Figure** 48: Von Mises stress [Pa], v=50m/min d=0.1mm

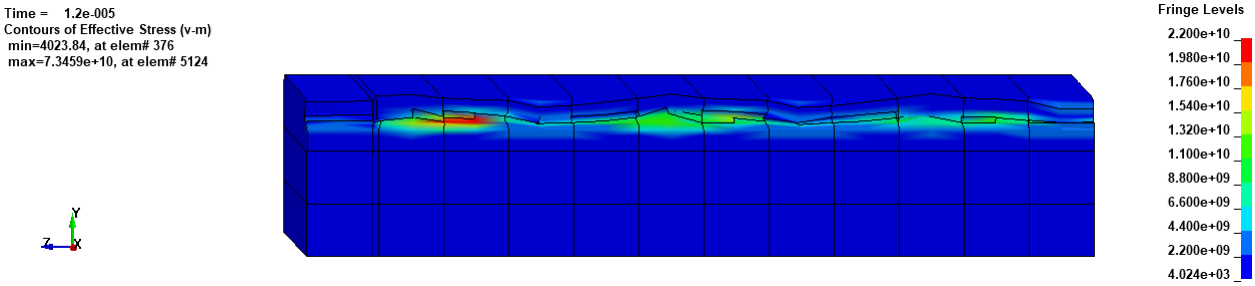


**Figure** 49: Von Mises stress [Pa], v=200m/min d=0.05mm

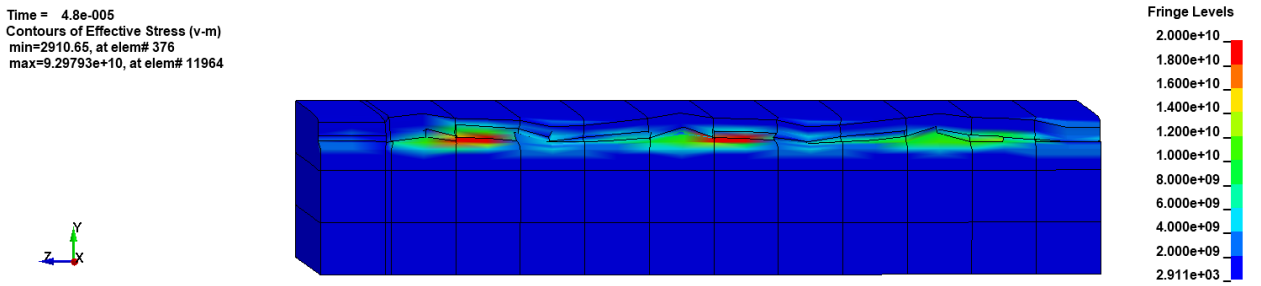


**Figure** 50: Von Mises stress [Pa], v=50m/min d=0.05mm

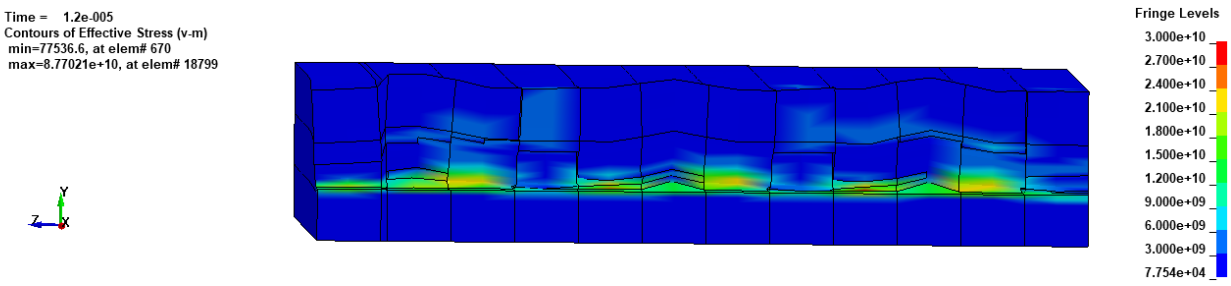


**Figure** 51: Von Mises stress [Pa], v=200m/min d=0.2mm

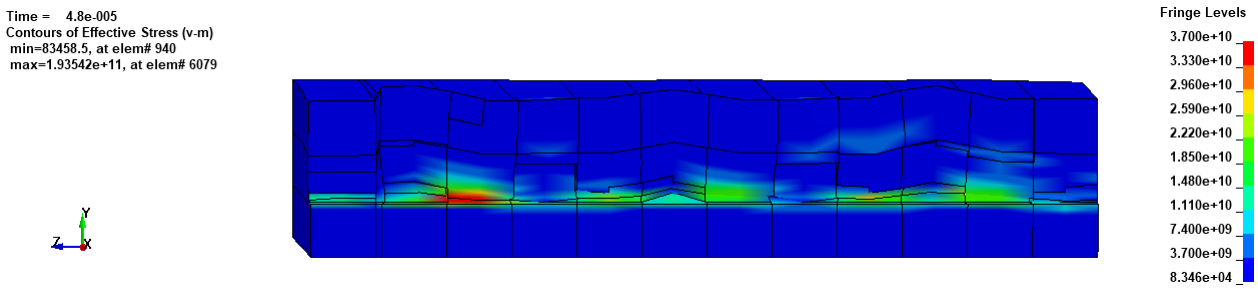


**Figure** 52: Von Mises stress [Pa], v=50m/min d=0.2mm

After observing the contours it can be appreciated that in all cases Von Mises stress is higher when the velocity is 200m/min. There is a direct relation between the depth of cut and the tension. This means that, regarding stress, the cases machined at higher speed are more likely to suffer breakage.

The same as for the velocities happens with the depth of cut. There is also a relation between the amount of material machines and the stress accumulated. In this case the contours showing d=0.2mm are the ones with a higher concentration. Therefore, the optimum is to cut smaller partitions.

Finally, another conclusion that can be achieved is that in all the cases the plies 3, 7 and 11 are the ones in which stress is concentrated the most. These plies have the same direction, so it is possible to state that stress affects more to the plies in which the direction of the fibre is 90°.

### Compressive and tensile stress

Another analysis is done but this time instead of comparing the different cases, different stresses are analysed. Therefore only one of the cutting conditions are selected: v=200m/min and d=0.1mm.

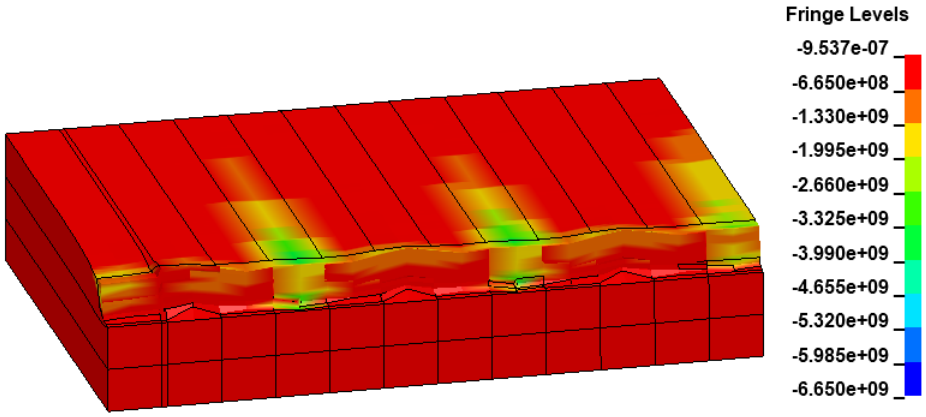


**Figure** 53: Compressive stress [Pa] in x direction

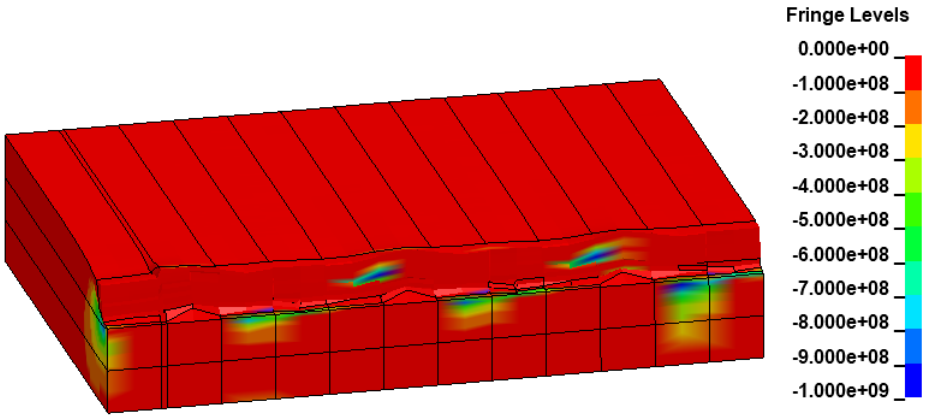


**Figure** 54: Compressive stress [Pa] in y direction

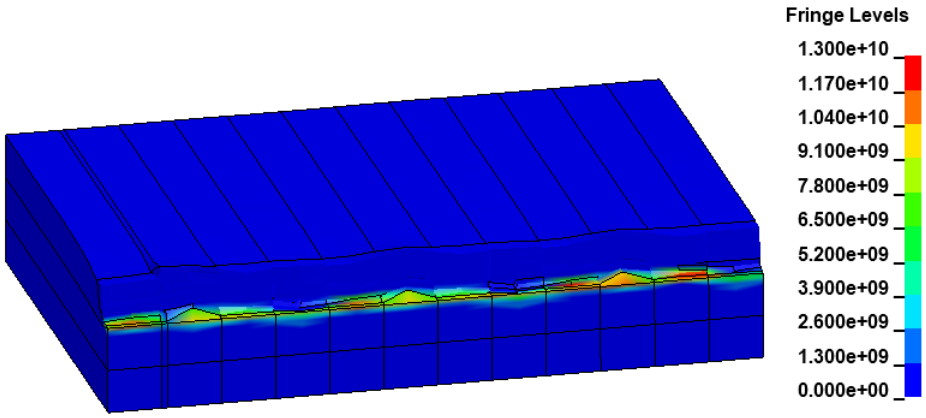


**Figure** 55: Tensile stress [Pa] in x direction

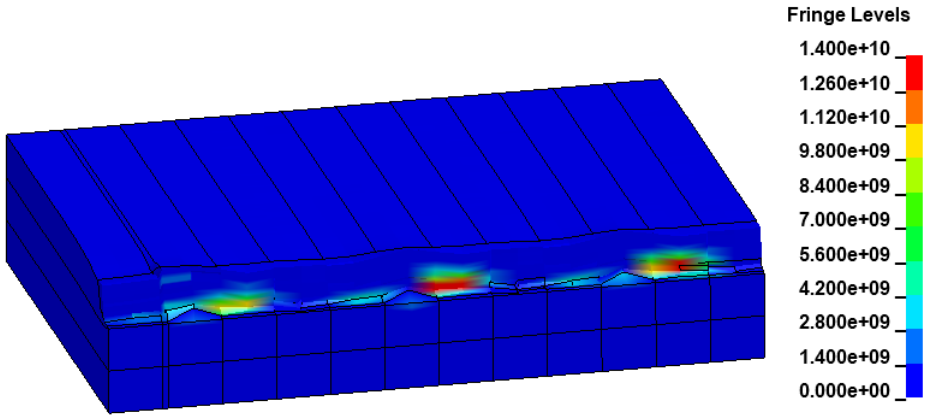


**Figure** 56: Tensile stress [Pa] in y direction

After observing the different contours, it can be appreciated that, in both compressive and tensile stresses, x direction reaches a higher concentration. This coincides with the tendency observed in the values gathered in Table 3. It also

fits with the character of the process, as during orthogonal cut the tool is moving along x axis, causing a more significant response in this direction.

It can also be stated that some fibre directions suffer more from one specific stress. In the case of compressive stress in x direction, the 0° direction plies are of especial interest as they are very likely to suffer failure if compressive forces are applied in the x direction. The same can be applied to the laminates in which fibre is oriented 90° when it is referred to the tensile stress in y direction. Therefore, it has been shown that this analysis allows to find the optimum combination of laminates with respect to the processing method.

### 4.2.3 Delamination

The main purpose of the model is to analyse the damage in the fibre and matrix. In this case the delamination between the first two plies is studied, as it is there where delamination is more likely to occur. A picture of the experimental sample for the test at the same conditions is included, so the concept of delamination and to show where it tends to appear (left picture) is clearer. Picture at the right shows the damage to the fibre and surface finish after the cut.

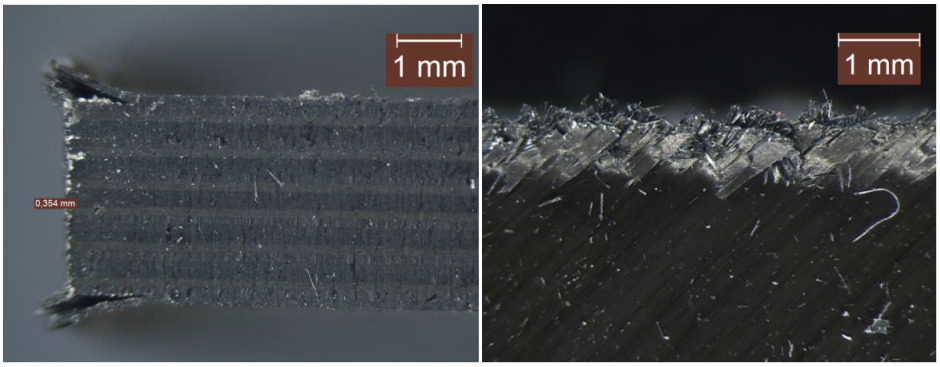


**Figure** 57: Experimental workpiece, v=200 m/min d=0.2 mm

First, in Figure 58 and 59 it can be observed how the cohesive element separates, becoming wider. In particular in Figure 59 it can be seen how at some point the purple element can be seen because the green one has been removed. The tool is placed above the green partition, so this element should be maintained, however if the software removed it is because it reached the maximum elongation, meaning that it is at this point where total delamination appears.

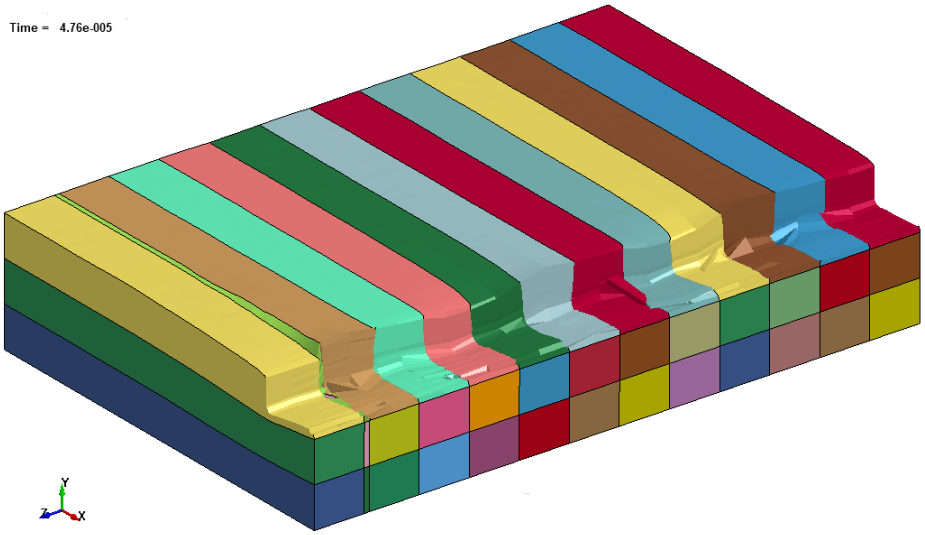


**Figure** 58: 3D model, v=200 m/min d=0.1 mm

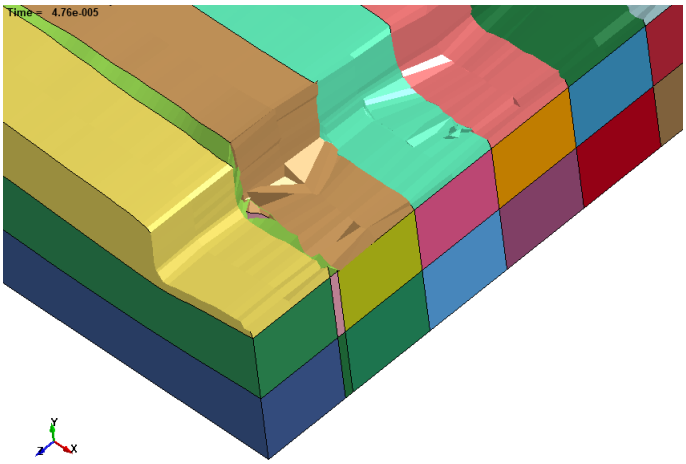


**Figure** 59: Zoom of the 3D model

3D model images of the cases with different depth of cut are also included. In Figure 60 the concept of delamination can be very well appreciated, it occurs in the part of the sample to be cut. However, the smaller the depth of cut, the less delamination damage appears.

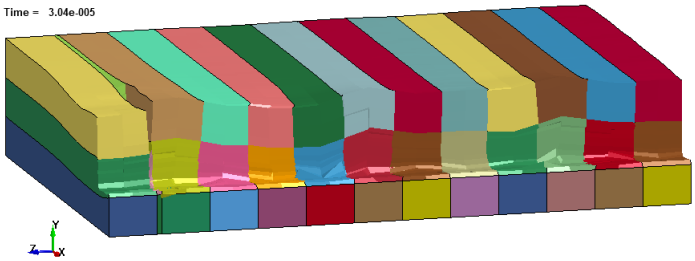


**Figure** 60: 3D model, v=200 m/min d=0.2 mm

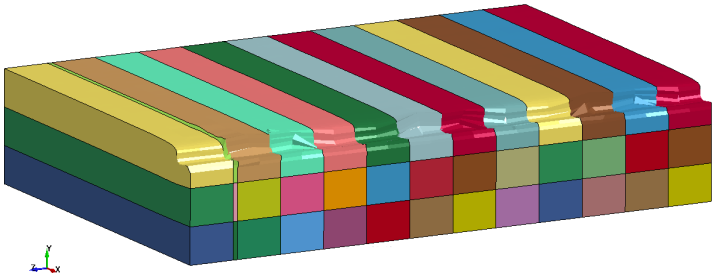

**Figure** 61: 3D model, v=200 m/min d=0.05 mm

Thanks to the accuracy of the numerical method it is possible to measure the length of the cohesive part at the same distance cut and in the cutting edge. The results were plot in Figure 62, and they show the dependency of the delamination with respect to the depth of cut and the velocity.

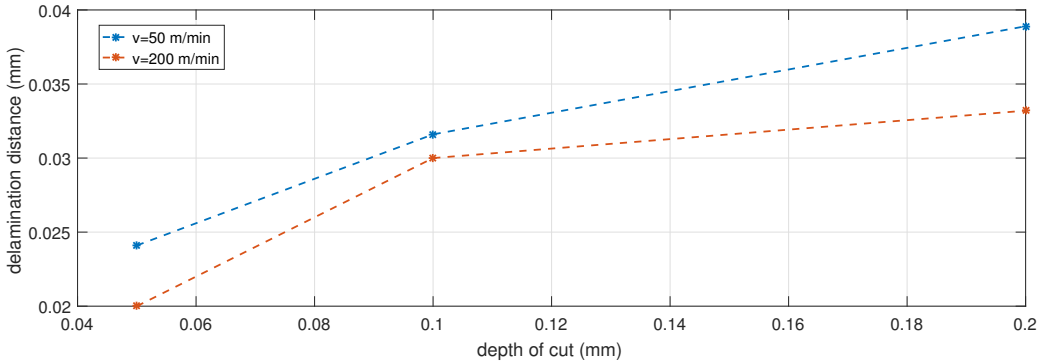


**Figure** 62: Relation of delamination with velocity and depth of cut

It can be observed that for the cases in which the velocity is 50m/min the delamination produced is higher, especially in the case of depth of cut 0.2. It is also proved what stated before, that delamination is directly proportional to the depth of cut.

This conclusion fits with the preferences of the industry, as the most common option is to machine at high-speed. However, in this numerical model the temperature effects are not included and in case of high speed they lead to high temperature affecting the composite material.

Finally, it can be stated that the optimum cutting condition based in delamination is v= 200 m/min and d=0.05 mm. It reduces damage in the composite material avoiding failure and leading to a longer lifetime.

### 4.2.4 Tool damage

In the experimental case the tool did not suffer any damage as observed in Figure 63. Nevertheless, one of the advantages of the FEM model is that the parts of

the tool that suffer the most can be analysed by displaying fringe component data on the model. The cases in which the velocity is higher, v=200m/min, have been selected as the force is also higher and therefore it is easier to appreciate the most damage place.

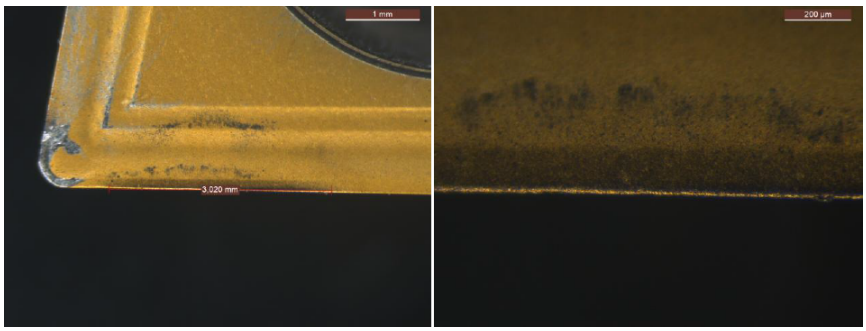

**Figure** 63: Tool damage

In Figure 64, it can be seen that the tool is not deformed or damaged at any point due to its hardness, but this does not mean that stress is not present. This picture shows the pressure during the simulation in the whole tool. The magnitude is not of importance as it is the pressure at a given time at the beginning (as the simulation is stopped due to computational time) and not the total pressure suffered. The units are in SI, therefore pressure is measured in Pascals.

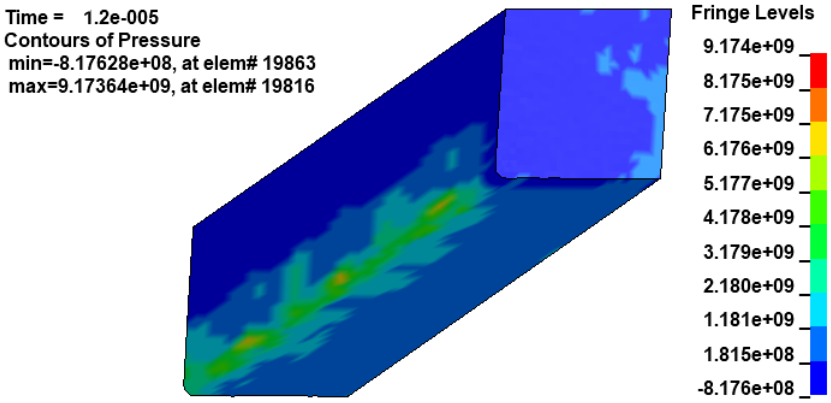


**Figure** 64: Tool pressure [Pa], d=0.1 mm

The same scheme for the other two depths of cut is shown in Figure 65 and 66. As expected, the cutting edge is the part where most of the damage appears and the tool used for a depth of cut of 0.2 mm reaches a higher concentration of pressure in comparison with the other two.

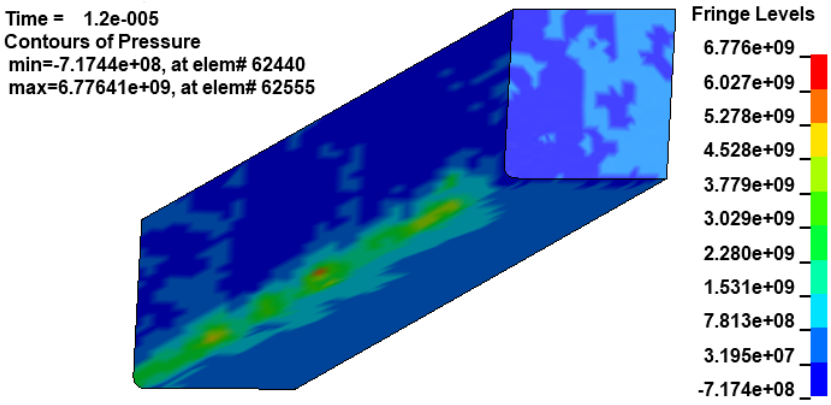


**Figure** 65: Tool pressure [Pa], d=0.05 mm

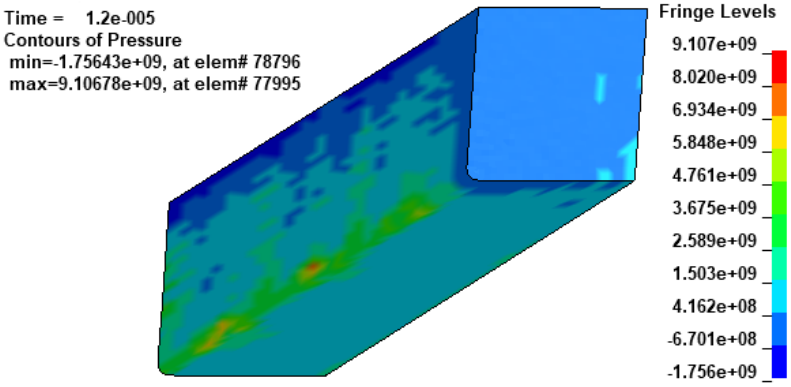


**Figure** 66: Tool pressure [Pa], d=0.2 mm

In the figures it can be appreciated that the part where damage is higher is concentrated in the cutting edge. The cutting edge of one of the sides of the tool is always with the minimum stress because the tool was larger than the sample in the xy plane were the symmetry is not applied. Stresses appear along the whole tool but there is a critical point in the center, better appreciated in Figure 66. Although in this case damage does not appear, when tools are not as rigid as the selected one it has to be careful as pressure increases and therefore, there is a probability to suffer abrasion and wear.

# 5 Socio-economic impact and legal framework

## 5.1 Socio-economic impact

During the thesis it has been exposed repeatedly the importance of FEM as it reduces the cost and operational time. It has a especial impact when simulating composite components as the material is more expensive than the traditional ones. However, although it is cheaper than building prototypes and testing them, it also has a cost. An approximate budget is presented in Table 12. It has to be considered that the licenses are paid only once and then software can be used for many models. All resources were provided by the university.

| **Personnel** | |
|---|---|
| Total engineer hours (h) | 300 |
| Salary (€/h) | 25 |
| **Licenses** | |
| LS-DYNA (4 months) | 6000 €/year |
| ANSYS multiphysics (4 months) | 30000 €/year |
| Matlab (2 months) | 800 €/year |
| **Total** | 19633.33 € |

**Table** 12: Budget

## 5.2 Legal framework

Regarding the legal framework, the European standard ECSS-E-HB-32-20 Part 4A [13] about composite machining for aerospace applications affects this project, as it defines some guidelines to guarantee quality results that need to be be fulfilled in the numerical model as well.

Moreover, from a more general point of view, this thesis is included in the context of machining CFRP in the aerospace sector. Therefore, the machining is intended to be a part of the manufacturing process of, for example, aircraft components. Therefore, the safety factor required in this industry has to be considered when computing the loads. Federal Airworthiness Regulation states that "Unless otherwise specified, a factor of safety of 1.5 must be applied to the prescribed limit loads which are considered external loads on the structure." So that, in case this model is used to simulate a cut in a actual part of the aircraft, the mentioned part must fulfilled the criteria established for the industry after the machining is performed.

# 6 Conclusions and future projects

## 6.1 Conclusions

A numerical model of an orthogonal cut in a CFRP has been created by using LS-DYNA. In order to validate it the results have been compared with experimental data at the same conditions. The following ideas can be concluded:

- The mesh directly affects the results achieved in the numerical method. A good election reaching a compromised between accuracy and computational time is required.
- The model is validated with respect to the principal force for different velocities but for the same depth of cut. The fact that for different depths of cut the principal force does not correspond with the experimental data can be explained as the failure criterion is not strict enough. It can be also attributed to the importance of the thermal effect in this machining process, which is not accounted in this numerical model. A higher temperature leads to a softer behaviour of the material and directly affects the forces.
- The tendency of the force with respect to the different velocities is maintained despite the depth of cut selected. Therefore LS-DYNA shows a realistic behaviour regarding this aspect.
- Thrust force was not considered in order to validate the model. However a comparison was done concluding that this model cannot be used to compute the force normal to the cutting plane.
- A stress analysis was done leading to the conclusion that laminates oriented at 0° were critical with respect to compressive forces in x direction, while laminates oriented at 90° are critical with respect to tensile forces in y direction. The highest Von Mises stress concentration is found in cases the cases with a bigger depth of cut and a higher velocity.
- Delamination can be appreciated thanks to the cohesive partitions implemented. It has been also shown that delamination has a greater effect in the case of a bigger depth of cut. The optimum conditions in order to avoid delamination has been selected as the highest speed, v=200 m/min, and the smaller depth of cut, d=0.05mm. Although delamination can be seen, it is hard to model the matrix cracking and fibre breakage to be observed.
- The tool damage can be precisely located thanks to the 3D FEM although no deformations appear due to its hardness. It is located the critical point in the tool, reaching a considerable higher pressure at the middle.
- It was possible to create the model in the software chosen, LS-DYNA, although some setbacks were found and the software elections were changed many times. One of the main drawbacks of the selected software is the computational cost, as for accurate results the time required was considerable.

## 6.2 Future projects

Now some ideas for future works are presented with the objective of improving this bachelor's thesis:

- Implement thermal effects in the same model so it can be observed the effect of the temperature field. the dependencies with respect the cutting speed can be studied, as well as the effect in the final sample.
- Implement more cohesive layers in order to analyse delamination at different plies.
- Create a numerical model in another FEM software in order to compare the results. ABAQUS can be an option and it can be observed if in this case the model is valid for different depths of cut. The computational cost of both softwares can be also studied a a key factor to select one of them, as it is of high importance in numerical simulations.
- With the validated model, perform an analysis of an orthogonal cut in composite with different laminates and compare them with experimental results.
- To simulate the matrix cracking and fibre breakage and implement a more strict failure criteria.

# References

[1] Composite lab, 'Composite vs Aluminium', 2016 URL: http://compositeslab.com/composites-compared/composites-vs-aluminum/

[2] Aerospace Materials I notes, Dpt. Materials Sci. and Eng. and Chemical Eng. UC3M, Spain.

[3] Carbonovus, Composite materials advantage and characteristics. Available: http://www.carbonovus.com/en/materiali-compositi/vantaggi-e-caratteristiche/

[4] Materials notes, 'Material selection and processing', University of Cambridge, available: http://www-materials.eng.cam.ac.uk/mpsite/interactive_charts/strength-density/basic.html

[5] Potter, Kevin (1996). An Introduction to Composite Products: Design, Development and Manufacture. Springer, 5th Ed. Chapman & Hall, London.

[6] F.París 'A study of failure criteria of fibrous composite materials' George Washington University, 2001 Available: https://ntrs.nasa.gov/archive/nasa/casi.ntrs.nasa.gov/20010035883.pdf

[7] LS-DYNA Keyword user's manual Volume II - Material Models, August 2012, Livermore Software Technology Corp.

[8] R.A.M. Santos, P.N.B. Reis, F.G.A. Silva, M.F.S.F. de Moura, Influence of inclined holes on the impact strength of CFRP composites, Composite Structures, Volume 172, 2017, Pages 130-136, ISSN 0263-8223, https://doi.org/10.1016/j.compstruct.2017.03.086.

[9] ICICI Securities 'Lightweight Composites: Vital cog in the CO2 emission reduction blueprint', 2015 Available: http://content.icicidirect.com/mailimages/composites.htm

[10] López de Lacalle Marcaide, Luis Norberto: 'Mecanizado de alto rendimiento', Ediciones Técnicas Izaro (2004)

[11] Kılıçaslan, Cenk. 'Modelling of metal cutting by finite element method.', Msc Thesis, Turkey, 2009.

[12] G. Raba Serrahimina 'Parametric study of the orthogonal cut machining in composite materials', Bachelor's thesis supervised by V.Criado del Álamo, UC3M, 2017.

[13] ESA Requirements and Standards Division, ECSS-E-HB-32-20 Part 1A. Structural materials handbook - Part 1: Overview and material properties and applications. 20 March 2011.

## Bibliography


1. J. L. Cantero, J. Díaz-Álvarez, M. H. Miguélez and N. C. Marín, "Analysis of tool wear patterns in finishing turning of Inconel 718," Wear, vol. 297, (1), pp. 885-894, 15 January 2013, 2013. DOI: https://doi.org/10.1016/j.wear.2012.11.004.

2. Aerospace Materials I notes, Dpt. Materials Sci. and Eng. and Chemical Eng. UC3M, Spain.

3. G. Raba Serrahimina 'Parametric study of the orthogonal cut machining in composite materials', Bachelor's thesis supervised by V.Criado del Álamo, UC3M, 2017.

4. Manufacturing Processes for Advanced Composites , F.C. Campbell, Elsevier, 2003 ISBN: 978-1-85617-415-2

5. LS-DYNA Keyword user's manual Volume II - Material Models, August 2012, Livermore Software Technology Corp.

6. LS-DYNA Keyword user's manual Volume I, May 2007, Livermore Software Technology Corp. Available:$http://lstc.com/pdf/ls-dyna_971_manual_k.pdf$

7. D. Aleksendrić and P. Carlone, "1 - introduction to composite materials," in Soft Computing in the Design and Manufacturing of Composite Materials, D. Aleksendrić, and P. Carlone, Eds. Oxford: Woodhead Publishing, 2015, pp. 1-5.

8. Fundamentals of composites manufacturing : materials, methods, and applications , Strong, A. Brent, Society of Manufacturing Engineers, 1989

9. N. Feito, J. López-Puente, C. Santiuste, M.H. Miguélez, Numerical prediction of delamination in CFRP drilling, Composite Structures, Volume 108, 2014, Pages 677-683, ISSN 0263-8223, https://doi.org/10.1016/j.compstruct.2013.10.014.